



University of Padova

Department of Agronomy, Food, Natural Resource, Animals and Environment

Master's degree in Sustainable Agriculture

LM69 – Scienze e Tecnologie Agrarie

Remote-sensing applications for biomass estimation in mountain grasslands

Supervisor

Prof. Cristina Pornaro

Co-supervisor

Prof. Stefano Macolino

Elena Basso

Daniele Pinna

Submitted by

Dario Agatino Giuffrida

The academic year 2023-2024

INDEX

Title	Page n°
Abstract	4
Introduction	5
Aim of the study	31
Materials and Methods	32
Results and Discussion	43
Conclusions	55
Bibliography	61

1. ABSTRACT

Mountain grasslands are largely known for livestock production, but they also supply essential ecosystem services. In recent decades, they have experienced degradation due to natural influences and anthropogenic factors. As a result, monitoring activities become crucial for assessing their health and productivity. Aboveground biomass (AGB) is a key parameter for evaluating grasslands quality and as a proxy for ecosystem functioning. Its estimation has been studied for many years using remote sensing reflectance and vegetation indices (VIs). This research intends to evaluate the relationships between VIs and dry matter production, and how the use of high-resolution satellite data and geospatial analysis techniques can enhance the ability to monitor and manage mountain grasslands, providing valuable information for agricultural production, conservation efforts, and habitat management. The experiment was conducted in 2023 at Malga Carriola, a temporary agro-zootechnical site in Caltrano (Vicenza). Twenty-three botanical surveys recorded all plant species and their abundance, to draw a vegetation map of the grazing surface. The obtained matrix of species was subjected to hierarchical cluster analysis. Furthermore, a random selection of 130 points was performed, followed by plant height measures in July 2023 using a Rising Plate Meter. Grass was harvested in 1 m² units, dried, and weighed to assess the dry matter (DM). Dry Matter and vegetation height were then correlated with remote sensing data. Raster imagery from Google Earth Engine (Sentinel-2 data), focused on the NDVI Normalized Difference Vegetation Index (NDVI) and the Normalized Difference Thermal Index (NDTI) as key VIs for this research. Raster images were therefore imported into GIS for a full visualization of VIs' trends, and for creating an attribute table for ANOVA to test the cluster analysis effect on DM and vegetation height. Despite previous research indicating a relationship between VIs and DM production, this research did not show any significant correlation. This study demonstrates the complexity of using NDVI and NDTI for AGB estimation in this area, suggesting that other factors can be involved in determining vegetation production and distribution. However, an accurate biomass estimation should include long-term monitoring and all plant growth stages. Moreover, integration of additional variables, testing multiple remote sensing platforms, and utilizing multiple VIs, can be important for defining accurate vegetation assessments, resulting in enhanced grassland protection activities.

2. INTRODUCTION

2.1 Grasslands

Grasslands are one the most widespread vegetation types all over the world (Latham et al., 2014; Ronchi et al., 2019) covering over 30% of the global land area (Shoko et al., 2016; Wang et al. 2019), equivalent to around 68% of the world's agricultural areas (Bazzo et al., 2021), and their net primary production (NPP) represents approximately 20% of total terrestrial productivity (Scurlock et al, 1998; Yunxiang et al., 2019).

Grasslands are typically known for livestock production, especially in areas where the typical agricultural activities are not feasible and/or where livestock and its products (milk and meat) represent the main economic sector for supporting livelihoods (arid and semi-arid regions) (Meshesha et al, 2020). They are very important for supplying essential ecosystem services, such as maintaining plant and animal biodiversity, regulating climate change and terrestrial carbon cycle, hydrogeological stability, and landscape conservation (Wang et al. 2019; Ronchi et al., 2019).

Grassland types:

- a) Human-generated grasslands (or improved grasslands): they derive from the human conversion of natural landscapes (i.e. forests) into pastures or grassland paddocks (Foley et al., 2005; Hill 2004; Ali et al., 2016). They are characterized by intensive management practices aimed at maximizing the production of animal-based products (i.e. dairy, meat, wool). Some of the most common management strategies include controlled fertilization, controlled grazing, and cyclic reseeding. These grasslands are very common in Northern Europe, New Zealand, and Australia (Foley et al., 2005; Hill et al., 2004; Ali et al., 2016).
- b) Highly managed natural grasslands: they include natural grasslands that have been intensively modified and managed to support livestock grazing. These areas have management practices similar to improved grasslands but aimed to preserve a higher level of natural vegetation composition (Hill et al., 2004; Ali et al., 2016).

- c) Rangelands: they are distinguished from pastures due to the presence of native herbaceous or shrubby vegetation, which is employed as a food source for domestic and wild herbivores.

Management of rangelands mainly consists of controlling the number of grazing units and the duration of the grazing season, in order to maintain an ecological balance. Examples of rangelands are tallgrass prairies in North America, steppes, shrub, woodlands, and savannas (Ali et al., 2016).

Pasture quality management and its implications

The importance of pasture goes well beyond the mere provision of food for animals, giving important contributions to ecological and environmental services; thus, the quality and quantity of pasture determine its overall value (Holmes et al., 2007; Pullanagari et al., 2013). However, the role of pasture's contribution to animal and environmental performance, and the relevance of measures of quantity/quality, will depend on the type and context of the farming organization (Pullanagari et al., 2013). The performance of grazing animals depends on how efficiently pasture energy and nutrients are obtained (Ulyatt, 1973; Pullanagari et al., 2013). Typically, pastures fed *in situ* already provide all the required nutrients and energy for the livestock, but supplemental feed may be necessary according to climate change effects, seasonal conditions and/or farm type. Forage quality is frequently assessed through chemical attributes like crude proteins, structural and non-structural carbohydrates, water, minerals, fiber content (ADF: acid detergent fiber; NDF: neutral detergent fibre), metabolizable energy (ME) and organic matter digestibility (OMD). Furthermore, a wide range of micro and macro constituents, as well as key physical attributes (i.e. species, proportion of green and dead material, presence of seed heads) have a direct influence on animal performance (Pullanagari et al., 2013). Besides forage quality, pasture management, including grazing frequency and intensity, plays a crucial role in manipulating both the quantity and quality of existing forage. As farming systems intensify and challenges increase, managing pastures becomes a more complex task that requires farmers to balance several drivers, in a constantly changing environment, while considering the overall short, medium, and long-term implications for animals and pastures performance (Pullanagari et al., 2013).

Environmental and ecological services are influenced by the pastoral system, its sensitivity to animal nutrition needs and environmental pressures. Understanding the role of different plant species, and vegetation components, is extremely important for both maintaining landscape integrity and serving as nutrient sources for animals. Moreover, pasture quality is crucial for enhancing system viability and sustainability as it significantly affects animal methane and nitrous oxide emissions (Holmes et al., 2007; Pullanagari et al., 2013).

Grassland degradation

In the last few decades, grasslands have experienced degradation due to natural factors (i.e., drought, wildfires) (Le et al., 2016; Zhou et al., 2005; Wang et al., 2019), anthropogenic factors (i.e. overgrazing by livestock, pollution) and an overall lack of monitoring and management practices (Harris, 2010; Qin et al., 2021). Furthermore, grasslands are vulnerable to climate change and threatened by invasive plants and woody plant encroachment (Cleland et al., 2006; Greer et al., 2014; Wang et al., 2019). Grassland degradation negatively affects forage and livestock production and the associated social-economic functions (Kwon et al., 2016; Wang et al., 2019). Rural populations emigrating to cities, and the abandonment of traditional agricultural methods (i.e., grazing, haymaking) have led to a reduction in active management of these areas. No human intervention often means invasion of alien species competing with the native ones, reducing the overall variety of plants and animals. Similar negative results can also be reached with the introduction of new agricultural practices and heavy machinery that, if not properly used, can result in overgrazing and/or soil compaction. Overtourism is another phenomenon that is increasingly impacting mountain areas: roads, accommodation facilities, outdoor activities, and noises that can disturb wildlife and lead to habitat loss. As a result, it is crucial to provide proper management practices to safeguard grasslands' health and productivity.

2.2 Aboveground biomass

Aboveground biomass (AGB) refers to the entire mass of living plant material and structures (i.e. leaves, stems) and it is a key biophysical parameter used to characterize grassland conditions and land degradation processes (Baghdadi et al., 2016; Qin et al., 2019). Aboveground biomass also corresponds to the herbivore-carrying capacity in pasture areas, so the maximum number of livestock that can graze on pasture for a given period without compromising the future production capacity (Qin et al., 2019; Chen et al., 2021). Monitoring and estimating AGB is essential for evaluating grasslands quality and functions and to improve management methods. Furthermore, it can be used as proxy for ecosystem functioning, ecosystem productivity, and biodiversity, helping managers and farmers understand the desertification and degradation process, and comprehensively evaluate carbon stocks (Qin et al., 2019; Yan et al., 2013).

2.3 Spatial-temporal variation of Aboveground biomass

Anthropogenic activities and policy

Human activities have a great impact on biomass distribution and change trends. Practices like land management, agricultural and forestry activities, as well as urbanization, can drive temporal changes in biomass distribution. For example, agricultural intensification may increase biomass through fertilization and irrigation, while urban expansion may lead to biomass loss through deforestation and habitat conversion. Different regions under different human conditions and activities show variations in AGB distribution (Shein et al., 2018). Effective policies and management can have a severe impact on biomass resources. Establishing nature reserves, land-use planning and zoning, implementing forest and grassland protection policies, developing climate change mitigation strategies, and enhancing public awareness on the ecological benefits, would have a powerful effect on the spatial change of biomass (Shen et al., 2018). With regards to pasture management, animal grazing practices are critical in affecting biomass availability. The choice among practices like continuous grazing, rotational grazing, cell grazing and many others, results into different intensities, duration and timing, with direct consequences on biomass production, vegetation recovery, soil fertility and biodiversity (Pullanagari et al., 2013).

Topographic and climatic influences

- Altitude and topography
 - Temperature gradient: with increasing altitude, temperature decreases due to alterations in atmospheric pressure and air density. Lower elevations are typically associated with warm temperatures, promoting high rates of evapotranspiration (evaporation + transpiration); higher elevations, on the contrary, have cooler temperatures, with subsequent moisture retention.
 - Precipitation patterns: in relation to landscape, orographic features, and the patterns through which air masses are forced to rise and cool as they encounter mountains or slopes, condensation of the water particles occurs, leading to precipitation. Low elevations usually have dry conditions, while at higher altitudes there is the tendency to have more frequent rain events. Better hydrothermal conditions positively influence plant species establishment (Zhang et al., 2011; Shen et al., 2018).
- Slope
 - Slope aspect: it refers to the compass direction that a slope faces (north, south, west, east). This is a critical element that affects the amount of sunlight received by a slope, which in turn affects sunlight exposure, temperature and moisture levels (Flores et al., 2009; Shen et al., 2018). Typically, north-facing slopes receive a small amount of sunlight, so they tend to be cool and moist; while the south-facing ones receive more direct sunlight and so tend to be warmer and dryer. This has direct consequences on the vegetation composition and biomass distribution, as climatic variability on slopes can support diverse habitats and species groups.
 - Terrain stability and water erosion: the steeper the slope, the less the vegetation concentration and biomass, since the slope influences the water drainage and its availability in the soil, plus it is directly responsible for soil erosion and soil loss (Shen et al., 2018).

Plant species and growth stages

Biomass estimation must consider the composition and the variety of plant species, including the different growth habits and phenological patterns. Different species show specific relationships between their structural properties (i.e. height, diameter) and biomass. Variations in species can correspond to variation in biomass density and Leaf Area Index (LAI). Leaf Area Index is defined as one-half total (i.e. one-sided) green leaf area per unit of ground surface area, and it is an important ecophysiological variable to represent vertical density of vegetation. Different plant species show different LAI, affecting their light interception and biomass production (Li et al., 2010).

An accurate biomass estimation also includes the knowledge of the plant growth stages. Especially for the employment of optical sensors, spectral data and values vary according to the proportion of biomass allocated in the different organs of the plant, as well as the chlorophyll content and dry matter (Casanova et al., 1998; Li et al., 2020).

Depending on the plant stage (i.e. germination, establishment, vegetative growth, tillering, heading, flowering, seed setting) biomass estimation can be subjects to errors. Normally, measurements are more accurate for growth stages before heading (pre-heading), while the results could be significantly poorer for growth stages after heading (post-heading) due to the spectral saturation under high biomass conditions. Overall, during the early vegetative stages, plants allocate most of their biomass to the above-ground structures (i.e. leaves, stems) in order to maximize their physiological activities related to photosynthesis, water and nutrient uptake. In late vegetative stages, including senescence and dormancy - on the contrary - above-ground biomass decreases to favor its accumulation in underground structures and storage organs (i.e. roots, rhizomes). During the reproduction stage, instead, most of the biomass is allocated in flowers, fruits, and seeds (Cheng et al., 2017; Fu et al., 2014; Wang et al., 2019; Li et al., 2020).

Seasonal changes

Seasons play an important role in affecting vegetation dynamics and so in biomass estimation. Specific times of the year correspond to precise phenological stages, impacting on biomass allocation and accumulation. Usually, peaks of biomass are related to the vegetative phases, in which plants grow and actively perform photosynthesis.

On the contrary, the frequent presence of senescent or dead plants during summer, and the low vegetation cover, reduce the amount of biomass detectable (Carpintero et al., 2020). It is also important to consider that each season, depending on the region, has specific climate condition, so when it comes to use remote sensing imagery for AGB estimation, clouds, rain, and snow are limiting factors (Chen et al., 2023). Seasonal changes also affect LAI, which normally increases during the growing season (spring-summer) as the plant and the canopy cover expand, then reaches a peak and subsequently declines during senescence (Li et al., 2020). Moreover, seasons drive the precipitation patterns and so the water availability for plants, affecting their health and physiological functions, as well as biomass production (Carpintero et al., 2020).

2.4 Grassland monitoring

It is essential for assessing their health, efficiency in productivity and the environmental impacts. Grassland monitoring methods are typically categorized into two groups: (i) ground-based and (ii) remote sensing methods.

Ground-based measurements

They rely on *in situ* data collection stations, measurement devices, and frequent field surveys (DelPozo et al., 2006; Ali et al., 2016). The most used methods for checking on grassland biophysical parameters are:

- Visual assessment: it is a non-destructive technique that consists of a visual inspection by human observers, typically experts or farmers. It is fast and cheap, but it is spatially sparse, and it has limited performance across different management strategies, leading to vague estimations (Newnham, 2010; Ali et al., 2016).
- Biomass sampling: it is a destructive method that involves harvesting grass samples from the site of interest, then drying (in specific ovens or sundried) and weighting to determine dry matter (DM) yield. Additionally, there could be laboratory assessments to evaluate grass quality and nutrient status (Xie et al., 2009; Ali et al., 2016). It is more accurate than visual estimation, but can be highly time-consuming depending on the number of samples to be used.

- Rising Plate Meter (RPM): it is mechanical or electronic device that consists of a handle and a plate that slides over a shaft. When positioned over the pasture canopy, it measures the height of the compressed pasture material between the plate and the ground. The data of compressed height is then converted into pasture biomass data (kg DM/ha) using a calibration equation set according to pasture species and time of the year/season (Gargiulo et al., 2020). Rising Plate Meter is cheap, non-destructive and accurate but it is time-consuming and labor intensive (Castle, 1976; Haki et al., 2012; Hejzman et al., 2014; Ali et al., 2016). In recent years, RPM devices have become more advanced. Some examples are the Ultrasonic distance sensors used in devices such as the GrassHopper and the GrassMeter. In addition to handheld devices, there has also been the development of vehicle-mounted devices (i.e. Pasture Meter, Pasture Reader), which are able to monitor grass height while driving the vehicle through the center of a towing tunnel, where optical sensors detect grass height, which is then regulated to estimate AGB (Bareth et al., 2018; Bazzo et al., 2023). It's important to note that the minimum number of measurements required per paddock/plot at a given time (RPM readings) impacts the accuracy of biomass estimation, plus the influence of the walking pattern (routes) to use when taking the RPM readings can be determining (Gargiulo et al., 2020).
- Field spectrometry: reflectance spectra data are collected using a portable spectrometer typically held at waist height and calibrated against *in situ* samples. Field Spectrometry can be adopted through different platforms, including hand-held devices, UAVs (drones) or satellite-based sensors. The amount of AGB and the plant species can be discriminated using local field data or spectral libraries (Ali et al., 2016). Markets offer several choices of hand-held devices, which normally cover the visible (RGB), NIR, UV and sometimes the shortwave infrared regions (SWIR) of the electromagnetic spectrum. There are also multispectral and hyperspectral spectrometers able to combine spectral and spatial information, by acquiring images at multiple wavelengths simultaneously, with high spectral resolution and spatial coverage. Field spectrometry is non-destructive and highly informative (possibility to acquire many biophysical data), but it requires trained operators and post-processing activities (Ali et al., 2016). The most employed tools for plant characterization studies are Vegetation Indices (Vis) and Geospatial Information Systems (GIS).

Ground-based methods are effective for local-scale monitoring and essential for remote sensing studies, facilitating cross-validation and algorithm training (Xu et al., 2008; Ali et al., 2016), but they laborious and feasible only for small-scale assessments (Xu et al., 2008).

Remote-based measurements

The AGB estimation has been studied for many years using remote sensing reflectance and vegetation indices. Remote sensing consists of acquiring data about areas or objects from distance without any physical touch or direct contact with the element of the study. The main concept behind Remote Sensing relies on the interaction between electromagnetic radiation and the Earth's surface or atmosphere. Indeed, depending on the physical and chemical features, different materials reflect, absorb, or emit electromagnetic radiation in characteristic ways. In the past, traditional methods for AGB estimation were mainly through sample inventory, which showed many shortcomings such as having poor representation, being destructive to grasslands, time-consuming, laborious, and inefficient. Remote sensing technology has instead macro, dynamic, economic, and efficient advantages, which could make up for the inadequacies of the traditional methods (Schellberg et al., 2014; Qin et al., 2021)

- Optical remote sensors and satellites:

Remote sensing technology has been very influential in improving land observation and management decisions (Bastiaanssen et al., 2000; Qin et al., 2019). Grassland vegetation can be monitored with large extents and a fine time resolution, measured and assessed, as remote sensing technology provides spectral, temporal, and spatial information (Qin et al., 2019). There is a wide availability of optical remote sensors, such as AVHRR - Advanced Very High Resolution Radiometer (≈ 1 km), MERIS - Medium Resolution Imaging Spectrometer (300-1200 m); MODIS - Moderate Resolution Imaging Spectroradiometer (250/500 m), SPOT – Satellite Pour l'Observation de la Terre (10/20 m), Landsat satellites (30 m), Sentinel satellites (10/20 m), WorldView satellites (1,24 m) and other high spatial resolution satellite and airborne images (< 10 -m) (Bao et al., 2019; Qin et al., 2019; Wang et al., 2019). All these, and many more, provide the primary data sources for grassland vegetation estimation with multispectral, multi-temporal, and multi-spatial resolution.

Images are obtained from sensors (optical and/or radar) that are installed on different platforms. The choice of the most appropriate remotely sensed data for biomass estimation generally depends on the scale and the costs of research (Chen et al., 2021). Optical sensors are the most appropriate for extracting biomass data from simple and uniform pastures.

However, using high-spatial-resolution (<10 m) optical data from airborne and satellite platforms for large-regional-scale AGB estimation can be constrained by several factors, including:

- weather conditions can affect the acquisition of good-quality data;
 - the optical data captures the information mainly from the top of the canopy rather than the vegetation structure (Wang et al., 2019);
 - saturation of surface reflectance occurs at moderate to high vegetation cover (Wang et al., 2019);
 - source imagery being expensive to acquire;
 - lack of spatial coverage, low revisit time, and difficulties during data processing (Chen et al., 2021).
- Unmanned Aerial Vehicle (UAV):
Remote sensing using a low-altitude Unmanned Aerial Vehicle (UAV), also known as Remotely piloted aircraft systems, Unmanned aircraft systems, or simply Drones, offer opportunities for precise and frequent characterization of agricultural environments in an accessible way (Su et al. 2021; Han et al. 2018; Gano et al., 2021). They represent a quick, simple, and cheap tool for measuring and estimating biophysical parameters, and they are particularly important in experimental fields that are difficult to access and/or with less instrumentation facilities. The acquisition of visible and NIR imagery at high spatial, spectral, and temporal resolutions, which has been used in remote sensing for a few decades to characterize vegetation and for AGB estimation, is becoming possible on small areas at an unparalleled level of spatiotemporal precision, without the known limitations of satellite or manned airborne remote sensing (Shahbazi et al., 2014; Maes et al., 2019; Théau et al., 2021). Some of the main limitations in their use, however, are related to their low spectral resolution compared to satellite or airborne sensors, with the main consequence of affecting the accuracy of the AGB estimation.

Furthermore, it is crucial to set an effective flight planning to acquire high-quality data; so, factors like flight speed, flight path, altitude and number of flights, are essential to ensure adequate coverage and data quality (Théau et al., 2021).

- Machine Learning (ML):

The new generation of satellites and the increasing need for mining large amounts of data, as well as the understanding of their complex and non-linear interactions, has triggered the necessity of the use of Artificial intelligence (AI). Recent innovations in cloud computing platforms have also accelerated the development and the implementation of Machine learning (ML) approaches, which often have a higher level of accuracy than human-crafted rules and traditional statistical methods. ML aims to automatically extract information from data by using different computational and statistical methods. (Singh et al., 2022; Chen et al., 2021). These methods can manage data with high dimensionality and can map classes with complex features. In the last few years, ML has become a major focus of the remote-sensing literature, especially in combination with satellite observations for ecosystem monitoring. (Chen et al., 2021). Some of the most known and used MAL algorithms for AGB estimation are Support Vector Machine (SVM), Gradient Boosting Machines (GBM) and Artificial Neural Networks (ANNs). The main advantage of ML techniques over other conventional statistical approaches in vegetation monitoring is that they can assess complex non-linear dynamics between canopy reflectance perceived by satellite sensors and the ecosystem structure, without having any prior assumptions about the underlying processes or data distribution, and this becomes very beneficial when it comes to study terrestrial ecosystems where vegetation growth varies according to spatio-temporal patterns and due to several factors (i.e. climate, deforestation, topography) (Hansen et al., 2013; Ma et al., 2021; Singh et al., 2020). In such cases, integrating ML techniques with satellite data helps capture the complexity of forest ecosystems across different spatio-temporal scales. (Chen et al., 2021).

- Geospatial Information Systems (GIS):

GIS is a successful and well-known tool in several fields of study, such as analysis of habitats and agricultural fields, resource conservation, ecosystem evaluation, planning of land use sites, environmental disaster monitoring, etc. (Bharti et al., 2021). Some of the distinct benefits of geospatial technologies include spatial data collection and integration from different sources (satellites, aerial photography, soil maps, LiDAR-Light Detection and Ranging, etc.), data analysis (spatial interpolation techniques, proximity analysis, combination of data layers) spatial model creation and mapping (visual representation of the spatial distribution of the variables). GIS is a relatively cheap tool, fast, highly informative, and important for setting decision-making strategies.

However, some basic considerations must be acknowledged to determine reliable GIS outcomes:

- Random field visits to the pre and post-GIS samples zone are vital to determine GIS mapping precision;
- The value of GIS performance depends on the satellite/digital image employed in the study (resolution, altitude, revisit time, spectral bands);
- The collection of the system of object classification (digital vs. manual) can also affect the quality of GIS products;
- Structural accuracy evaluation using standard approaches such as error matrix computation (also known as uncertainty matrix) will improve the precision of the GIS performance (Bharti et al., 2021).

2.5 Vegetation Indices

Many systems seek to establish relationships between the radiation absorbed by the canopy and the biophysical attributes. In healthy plants, properly supplied with water and nutrients, there is a positive and linear relationship between the amount of photosynthetically absorbed radiation by the canopy and biomass production (Trentin et al., 2019; Barboza et al., 2023). Considering this, Vegetation indices (VIs) have been widely used thanks to their ability to predict and evaluate characteristics of vegetation cover.

Such information can be a valuable tool for farmers, land managers and research institutions, as it is helpful in decision-making, management, harvest planning, yield forecasting, and finally, information gathering and monitoring (Barboza et al., 2023). Vegetation indices, or Vegetation spectral indices, can be described as the arithmetic combination of two or more spectral bands related to the spectral characteristics of vegetation (Matsushita et al., 2007; Venacio et al.,2020). AGB estimation through VIs is possible because many of them provide a stable and near-linear estimate of accumulated absorbed photosynthetically active radiation, which represents the energy source for photosynthesis, that principally controls vegetation productivity, which is proportional to total AGB (Venacio et al.,2020).

Healthy canopies of green vegetation have a specific interaction with certain portions of the electromagnetic spectrum. Chlorophyll causes a strong absorption of energy, primarily for use in photosynthesis; this absorption peaks in the red and blue areas of the visible spectrum, while the green area is reflected by chlorophyll. Simultaneously, the near-infrared region (NIR) of the spectrum is strongly reflected through the internal structure of the leaves (Silleos et al., 2006). Vegetation indices are broadly used in both ground-based and remote-based measurements, and they are usually integrated with other systems or data (i.e. climate, land surface properties, topography, ecological indicators, LAI, etc.) to provide a deeper and comprehensive understanding of vegetation dynamics.

2.6 Ratio Vegetation Index

Ratio Vegetation Index is a basic vegetation index built on the principle that leaves absorb relatively more red than infrared light.

Formula: $RVI = R/NIR$

where: NIR is the near infrared band reflectance and
R is Red band reflectance

Its values range from 0 to positive infinity. Values close to zero are sign of sparse or low vegetation cover. Values greater than 1 indicate healthy and dense vegetation.

The RVI index is broadly employed for green biomass estimations and monitoring, particularly at high-density vegetation coverage, since it is very sensitive to vegetation and has a good correlation with plant biomass. However, when the vegetation cover is sparse (< 50% cover), RVI is too sensitive to atmospheric effects and its representation of biomass is weak (Xue et al., 2017).

2.7 Simple Ratio

Simple Ratio (SR) is another basic vegetation index calculated as the ratio of light scattered in the NIR and absorbed in red bands, which reduces the effects of atmosphere and topography. The range of values is from 0 to approximately 30.

Values close to zero indicate sparse or low vegetation cover, while healthy vegetation generally falls between values of 2 and 8 (Enkhtuya et al., 2022).

Formula: $SR = NIR / R$

where: NIR is the near infrared band reflectance and R is Red band reflectance

Its values are high for vegetation with a large leaf area index (LAI), and low for soil, water, and non-vegetated features. SR incorporates limited calculations, and since it simply compares reflectance in Red and NIR spectral bands (unlike other indices that employ multiple spectral bands), issues of high sensitivity of the index to changes in vegetation cover or structure can occur, especially in early stages of plant development. As the plant grows and evolves through the seasons, the canopy becomes denser, with higher chlorophyll content, and structurally more complex. All these elements can influence the timing of peak values for SR (Venancio et al., 2020).

2.8 Green-Red Vegetation Index

Green-Red Vegetation Index (GRVI) is a simple ratio index that uses the green and red bands to assess vegetation health. It is sensitive to leaf color change (leaf greening and autumn coloring) (Motohka et al., 2010)

Formula:
$$RVI = (Green - Red) / (Green + Red).$$

Its values range from -1 to 1. Negative values indicate non-vegetated surfaces (water bodies, snow, bare soil) or less healthy vegetation (stressed, damaged, attacked). Values close to zero are typical of low vegetation cover or sparse vegetation. Positive Values of GDVI indicate healthy and dense vegetation cover.

2.9 Normalized Difference Vegetation Index

Normalized Difference Vegetation Index (NDVI) is widely used in ecological research and farm management as a proxy for the quantity and quality of forage available to herbivores (Pettoirelli et al., 2011; Garrouette et al., 2016). NDVI calculates the contrast between RED wavelengths absorbed by photosynthetic pigments (i.e. chlorophyll), and NIR reflectance wavelengths scattered by leaf mesophyll cells (Edirisinghe et al., 2012, Garrouette et al., 2016).

Formula:
$$NDVI = (NIR - Red) / (NIR + Red)$$

The measurement scale has ranges from -1 to 1. 0 represents the approximate value of no vegetation or very sparse vegetation; values close to 1 indicate healthy and dense vegetation, while values close to -1 indicate non-vegetated surfaces (i.e., water bodies) (Silleos et al., 2006). The accuracy of NDVI for estimating AGB is acknowledged to be sensitive to scattering and elevated NIR irradiance from dense biomass, heterogeneous plant structure, senescent vegetation, soil exposure, topography, and atmospheric contaminants (Huete et al., 2002; Garrouette et al., 2016). In sparsely vegetated areas, variation in moisture and brightness of exposed soil increases the irradiance of the NIR band, and as a result NDVI estimates will be biased. Also, landscapes with different topographic characteristics, variation in the viewing geometry, sun elevation angle and surface albedo can severely affect NDVI.

Atmospheric contaminants were proved to bias NDVI estimates in wet climates and seasons than in dry climates and seasons (Gao et al., 2000; Tucker et al., 1977; Tittebrand et al., 2009; Garrouette et al., 2016).

As NDVI values have a limited dynamic range (-1 to 1), it can fail to accurately represent biomass variations in areas with highly dense vegetation, leading to issues of saturation. Furthermore, it is important to capture biomass dynamics during specific vegetative phases, since NDVI manifests saturation values typically during the reproductive stages of the plant, where variations in biomass are less detectable (Barboza et al., 2023). NDVI is also influenced by LAI. Indeed, at high LAI values, additional leaf biomass could contribute marginally to NDVI, leading to saturation as the canopy intercepts most incident radiation (Barboza et al., 2023).

Lastly, the time of year (season) and the farming practices have great effects on biomass and so on the NDVI (Edirisinghe et al., 2012). Typically, during early summer (June to July) there is a reduction in maximum biomass as fodder consumption by the livestock exceeds the daily pasture growth while in late summer (August and September) the trend reverses as higher daily temperatures lead to increases in pasture growth, allowing net accumulation. From October to December the range of both biomass and NDVI decreases, this is likely to be associated with the maturity of pastures and the cooler temperatures (Edirisinghe et al., 2012). Moreover, since the crude protein content and digestibility of vegetation decline with seasonal growth as fibrous cell wall structures accumulate, NDVI has also been shown to be correlated with the quality of forage for herbivores early in the season (Garrouette et al., 2016).

2.10 Transformed Normalized Vegetation Index

Transformed Normalized Vegetation Index (TNDVI) was born as an early improvement of the NDVI, developed specifically for arid and semi- arid rangelands (Rouse et al. 1974), however it does not include a soil line correction factor.

Formula:
$$\text{TNDVI} = \text{NDVI} + 1/2$$

TNDVI's values range from 0 to 1. Values close to 0 are typical of low vegetation cover or non-vegetated surfaces. Values close to 1 indicate healthy and dense vegetation cover.

Several studies confirmed TNDVI to be a good alternative to NDVI and a good proxy for AGB estimation, especially in presence of dry grass and shrubs, as it improves the ability to capture the variability in aboveground biomass in semi-arid rangelands and environments (Baghi et al., 2019). Indeed, in such conditions, vegetation cover tends to be sparse and randomly distributed, leading to skewed distributions in vegetation indices like NDVI. TNDVI accounts for these features and proposes specific corrections (i.e. histogram correction, normalization) (Baghi et al., 2019).

2.11 Normalized Difference Thermal Index

Normalized Difference Thermal Index (NDTI) is an index specifically designed to highlight temperature variances in a given area by comparing thermal infrared (TIR) bands. Already known in the context of urban heat island studies, it has been recently introduced for agricultural and environmental monitoring activities. Due to their differing thermal masses, the elements found in a given area (i.e., rocks, vegetation, wood, etc.) will heat and cool differently, and therefore their TIR signatures will differ. If materials have different spectral responses, then ratioing the significantly distinguishing bands and normalizing those values to a standardized range will provide a sensitive and comparable test of thermal character (McInerney et al., 2007). Thanks to transpiration and specific leaf physical properties, vegetation affects surface temperatures, cooling them down. In fact, high biomass levels are normally correlated with cooler surface temperatures, because dense vegetation tends to retain moisture and facilitate evapotranspiration process. By confronting two TIR bands. NDTI can two thermal infrared bands, can detect differences in surface temperatures, which can reveal changes in vegetation cover and biomass Furthermore, it can be effective in spotting bare soil and/or rocky areas. Soil and rocky materials show different thermal properties, heating up and cooling down much faster than vegetation (low thermal inertia).

Time of the day chosen for NTDI assessment is crucial: the temperature contrast between vegetation and bare soil is higher during the hottest part of the day (McInerney et al., 2008).

NDTI values range from -1 to +1:

- +1 = indicates the maximum positive difference between the two TIR bands. This would imply that certain types of materials emit more thermal radiation, resulting in warm surfaces
- -1 = indicates the maximum negative difference between the two TIR bands. This denotes that specific types of materials emit less thermal radiation, resulting in cool surfaces
- 0 = no difference exists between the two TIR bands, denoting the presence of materials with uniform temperatures

Formula: $NDTI = \frac{Band(x) - Band(y)}{Band(x) + Band(y)}$

where: Band(x) is the radiance value from the first thermal infrared band (TIR1).

Band(y) is the radiance value from the second thermal infrared band (TIR2).

TIR1 is a thermal infrared band with a 10.60 to 11.19 μm wavelength Range; TIR2 is a thermal infrared band with a 11.50 to 12.51 μm wavelength range (Seenipandi et al., 2021). Both TIR1 and TIR2 fall within the Long Wave Infrared (LWIR) range: 8 – 14 μm .

2.12 Enhanced Vegetation Index

Enhanced Vegetation Index (EVI) is an optimized vegetation index designed to enhance the vegetation signal with improved sensitivity in high biomass regions and improved vegetation monitoring through de-coupling of the canopy background signal and a reduction in atmosphere influences. (Somvanshi et al., 2020).

Formula: $EVI = G \times \left[\frac{NIR - Red}{NIR + C1 \times Red - C2 \times Blue + L} \right]$

EVI is a ratio of red and NIR reflectance (like NDVI), but it also incorporates an adjustment factor to account for the non-linear distortion from soil ($L = 1$), a blue band to reduce atmospheric contamination of the red band, and aerosol resistance coefficients ($C1 = 6$, $C2 = 7.5$), and a Gain factor ($G = 2.5$). (Liu et al., 1995; Huete et al., 2002; Garrouette et al., 2016). EVI is usually proposed as a more robust proxy for AGB and forage quality estimation than NDVI, thanks to its improved resistance to saturation, soil exposure, and atmospheric contamination; plus, it is more responsive to canopy variations, canopy type and architecture (Somvanshi et al., 2020). EVI's adjustments make it more robust than NDVI in areas with dense vegetation and high soil exposure, but at the same time make EVI more sensitive to variation in the viewing geometry, surface albedo, and sun elevation angle across variable terrain (Garrouette et al., 2016).

Mountainous terrains can pose challenges for biomass estimation, due to variations in slope, aspect, complex vegetation structure and shading effects, thus elevation changes, atmospheric conditions can vary rapidly. EVI is able to minimize these interferences.

Indeed, employing the blue-band in its calculations helps to reduce the overall background noise (the influence of non-vegetation elements such as rocks and soil), making EVI a reliable choice for biomass estimation (Garrouette et al., 2016; Boschetti et al., 2007). In dry and semi-dry rangelands (i.e., savannas) EVI has been shown to be the most suitable among VIs. However, its correlation with AGB can sometimes be only “moderate”, and this can be attributed to several factors, such as the presence of flowers, the type of plant species (grass), and their physical characteristics. Flowers, in particular, give a specific and high reflectance in the visible spectrum affecting EVI calculations and leading to saturation problems, without having the possibility of effectively discriminating the differences in grass biomass, nor accounting for factors like senescent or dry vegetation (Munyati et al., 2021).

2.13 Enhanced Vegetation Index 2

Enhanced Vegetation Index 2 (EVI2) works as a substitute of EVI. It consists of a two-band version of the EVI that simplifies the calculations by removing the blue band component, in addition it retains the soil-noise adjustment function, and maintains the improved sensitivity and linearity in high biomass regions (non-saturation) seen typically in EVI.

These goals are achieved by incorporating in its calculation a linearity-adjustment factor (β) derived from the linear vegetation index (LVI), enhancing sensitivity in high biomass regions (Jin et al., 2014; Jiang et al.,2008).

Formula:
$$EVI2 = G \times [(NIR - RED) / (NIR + C1 \times RED - C2 \times BLUE + L)]$$

The similarity between EVI and EVI2 was analyzed and validated at local and global scales. Global EVI2 images show very similar patterns as global EVI images, particularly in clear-sky conditions, and the differences between them were almost null. When aerosol or residual clouds are present, EVI is generally larger than EVI2 due to the aerosol resistance property of EVI. The consistency between EVI and EVI2 across various land cover types demonstrated that their similarity was independent of land cover. Time series (temporal) analysis further revealed their similarity was seasonally independent. (Jiang et al.,2008).

2.14 Soil-adjusted vegetation index

Soil-adjusted vegetation index (SAVI) is a modified version of NDVI and relies on the concept of the soil line which, in a bispectral scatterplot, usually depicts the Red and NIR channels, describes soil pixels with differing moisture content that form a line at the lower part of the scatterplot. Pixels with increasing vegetation cover will appear more distant from the soil line (Huete et al.,1988; Baghi et al., 2019). Also here, just like for EVI, a soil-adjustment factor “L” is proposed to account for first-order, non-linear, differential NIR and red radiative transfer through a canopy (Huete et al.,1988; Jiang et al.,2008).

Formula:
$$SAVI = [(NIR - RED) \times (1 + L)] / [(NIR + RED + L)]$$

The L factor changes with the reflectance characteristics of the soil (color and brightness), and its choice depends on the density of the vegetation one needs to analyze. The value of L ranges from 0 to 1. Normally, in cases of very low vegetation, the use of a L factor of 1.0 is suggested for intermediate 0.5, and for high densities 0.25 (Silleos et al., 2006). Environmental conditions like temperature, humidity, photoperiod, and precipitation, are directly or indirectly related to the time of the year, and changes in these factors affect plant growth rates and physiological processes, which in turn impact on the reflectance property of the vegetation.

SAVI incorporates complex calculations that make it able to capture the variations in canopy density, structure, and composition as the seasons evolve throughout the year, showing later timing of peak values (unlike other Vis such as SR) (Venancio et al., 2020). In terrains characterized by sparse vegetation or areas in which soil brightness varies significantly due to the presence of rocks (i.e., arid regions, mountainous regions) or man-made structures, SAVI index has shown good performances in correcting background noise as it mitigates the influence of soil reflectance on vegetation (Jin et al., 2014).

Several modifications have been made to the SAVI equation, leading to new indices like:

- Modified Soil-Adjusted Vegetation Index (MSAVI): it improves SAVI regarding the soil noise under heterogeneous soil background (Qi et al., 1994; Baghi et al., 2019). Its use is restricted to high vegetation density areas.
- Optimized Soil-Adjusted Vegetation Index (OSAVI): it enhances SAVI for flat terrains with relatively homogenous soil reflectance (Rondeaux et al., 1996; Baghi et al., 2019).
- Soil-Adjusted Vegetation Index (TSAVI): it minimizes soil brightness influences by assuming that the soil line has an arbitrary slope and intercept (Enkhtuya et al. 2022). It shows some resistance to high soil moisture, and it was specifically designed for semi-arid regions and does not perform well in areas with full vegetation cover.

2.15 Atmospherically Resistant Vegetation Index

Atmospherically Resistant Vegetation Index (ARVI) is generally used to remove the effects of atmospheric aerosols and ozone. It is mostly useful in regions with a high content of atmospheric aerosol, including tropical areas polluted with soot (Somvanshi et al., 2020). This index is based on the knowledge that the atmosphere significantly affects the Red band reflectance compared to the NIR reflectance (Xue et al., 2017).

Formula: $ARVI = [NIR - Red - y(Red - Blue)] / [NIR + Red - y(Red - Blue)]$

where: "y" is a quotient derived from the components of atmospheric reflectance in the blue and red channels.

Its values range from -1 to 1. Negative values indicate non-vegetated surfaces (water bodies, snow, bare soil) or less healthy vegetation (stressed, damaged, pest-attacked). Values close to zero are typical of low vegetation cover or sparse vegetation (Rondeaux et al., 1995). Positive Values of ARVI indicate healthy and dense vegetation cover. Apart from Red (0.66 μm) and the NIR (0.865 μm) bands, this index also uses the Blue band (0.47 μm). Compared to other indices, the resistance of the ARVI to the atmospheric effects is achieved by a self-correction procedure for the atmospheric effect on the Red band. To correct the radiance in the red channel, difference in the radiance between the blue and the red bands is done (Somvanshi et al., 2020).

When the study area reveals specific characteristics - in terms of atmospheric resistance properties - that are advantageous for ARVI's calculations, results show higher correlations with ground-based measurements of vegetation biomass or health compared to other indices like NDVI and SAVI. Indeed in case of proximity to water bodies, large areas and high atmospheric variability, ARVI is able to reduce the influence of factors like water vapor, aerosols and pollutants (i.e. haze, smog), and so of the atmospheric scattering and absorption, resulting in more accurate estimates of AGB. Furthermore, ARVI showed high sensitivity to variations in vegetation cover, so it can be used a good proxy for estimating biomass in landscapes with variable vegetation density (Bayaraa et al., 2021).

2.16 Fractional Vegetation Cover

Fractional Vegetation Cover (FVC) is defined as the ratio of the vertical projection area of above-ground vegetation organs to the total vegetation area. It represents a measure of vegetation density, ranging from 0% (no vegetation cover) to 100% (full vegetation cover). FVC can be relevant in the study of grassland health and vegetation cover changes over time (Li et al., 2022; Andreatta et al., 2022). Spatiotemporal drivers such as erosion, revegetation, disturbances, and climate patterns, can influence its measurements (Liang et al., 2020; Andreatta et al., 2022). FVC assessment includes data collection, preprocessing (atmospheric and geometric corrections), vegetation indices (VIs) and FVC calculation, FVC-VIs relationship analysis, and model validation.

Atmospheric correction is important for reducing the impacts of particles, pollutants, water vapor, and various gases on solar radiation. Methods such as the Quick Atmospheric Correction (QUAC) or the Dark Object Subtraction (DOS), which rely on ground data as reference points for calibration and satellite imagery for image acquisition, can be useful for accurate FVC measurements. Statistical methods such as regression analysis are therefore needed to establish any existing relationships between the ground and the satellite data (Johnson et al., 2012).

Field measurements of FVC are carried out using subjective visual estimation and several standardized sampling methods, which supply accurate ground references for remote sensing algorithm development (Liang et al., 2020; Andreatta et al., 2022). Visual estimation is typically based on the experience of the estimator, so it is highly subjective and random. Sampling methods such as Point-count and Needle sampling apply statistical principles in estimating vegetation presence with a high degree of accuracy. However, they are time-consuming and complex to carry out. Nowadays, digital photography classification is a much more efficient and objective way of estimating FVC, thanks to the improvements in technology and image quality (Li et al., 2022; Andreatta et al., 2022). Estimation of FVC is also successfully achieved through satellite imagery and the use of different systems: empirical models, pixel decomposition models, physical-based methods, spectral mixture analysis, and machine learning algorithms. (Xiao et al., 2016; Andreatta et al., 2022).

2.17 Statistical methods for data analysis and validation

Correlation analysis

Correlation analysis is a powerful method that measures strength and direction of the relationships between variables.

Some of the most adopted techniques involve:

- Bivariate correlation: it examines the strength and direction of the linear relationship between the dependent variable (biomass) and the individual predictor variables. For ordinal or ranked data, Spearman correlation coefficient (ρ) is largely used ; while Pearson's correlation coefficient (r) is the most suitable for continues variables. Pearson's coefficient values range from -1 to 1.

A positive correlation ($r > 0$) shows a positive linear relationship, while a negative correlation ($r < 0$) indicates a negative linear relationship. In general, values close to 1 indicate strong relationships; weak relationships if close to -1; weak or no linear relationship if close to 0 (Adame-Campos et al., 2019).

- Correlation matrix: A correlation matrix displays simultaneously the correlation coefficients between the dependent variable (biomass) and multiple predictor variables. This allows to identify potential predictors that are highly correlated with biomass and prioritize them for further analysis. They are useful for building prediction models for biomass estimation, facilitating decision-making processes.

The commonly used software packages for running correlation analyses are R and Python, with a large availability of libraries. Correlation is overall a strong and robust statistical method to identify how well the factors under study (climate factors, elevation, vegetation type, etc.) correlate with biomass levels. However, it shows important limits when it comes to knowing about the causal relationships among variables, thus it is not efficient in case of non-linear relationships. In these cases, regression analysis can be a valid alternative method (Enkhtuya et al., 2022).

Regression analysis

Regression analysis is one the most common, well-studied and easy-to-use technique for biomass estimation studies. It uses satellite-driven vegetation indices (VIs) in combination with *in situ* measurements (ground-collected biomass, fresh and dry) for developing regression models to relate biomass (dependent variable) to one or more predictor variables (independent variables) that are assumed to influence biomass (Chen et al., 2021). Regression analysis' results consist of an equation that describes how changes in the independent variables are associated with changes in the dependent variable, allowing the identification of which vegetation index presents the best correlation (Boschetti et al., 2006).

Regression models steps:

- *In situ* data mining;
- Data processing (data cleansing from errors and outliers);

- Selection of the appropriate regression model (linear, non-linear, Generalized Linear Models-GLMs, etc.);
- Model fit evaluation through different methods (R^2 , Adjusted R^2 , Root Mean Squared Error-RMSE, Mean Absolute Error-MAE etc.);
- Regression model validation (cross-validation, residual analysis, external validation).

The accuracy of the analyses depends more on the quantity and quality of the data from field samples than on the type of statistical regression (Morais et al., 2021; Bazzo et al., 2023).

Linear regression methods are largely known and employed for biomass estimation studies. Some examples are:

- simple linear regression (SLR): focuses on the linear relationship between one predictor variable and one dependent variable;
- multiple linear regression (MLR): linear relationship among multiple predictor variables and one dependent variable;
- stepwise linear regression (SWL): predictor variables are added or removed based on their significance;
- polynomial regression: incorporates polynomial elements (i.e. cubic);
- partial least squares regression (PLSR): mostly used for large dataset for reducing variables to smaller set of predictors.

Linear regression methods are preferred to non-linear regression models because of their simplicity, high interpretability, identification of the key factors influencing the object of the research (biomass), large availability of software and computational resources (R, Python), reliability, and robustness (Bazzo et al., 2023; Barrachina et al., 2014). However, they tend to be less performing when the relationship among dependent and independent variables is non-linear, as well as in case of complex interactions among the predictors (independent variables) (Porter et al., 2014; Lawrence et al., 1998). Unlike linear regression models, non-linear models such as exponential regression, Gaussian regression, logarithmic regression and others, are based on the fact that the relationship between variables is not linear but way more complex.

As these relationships are harder to explain, non-linear regression models provide more robust, flexible, and accurate infrastructures to represent these patterns and dynamics. Nevertheless, they result to be difficult in the use both conceptually and computationally, putting some challenges with regards of the interpretation of outcomes (high level of expertise is required) and overfitting (capture of random variability).

In recent times, other regression models are emerging as powerful tools in biomass estimation research. For example, Linear mixed models are proposed as improvements of simple linear models as they incorporate fixed factors and random factors and are particularly used for data with a hierarchical structure. Linear mixed models can explore the differences between the effects within and between groups (Qin et al., 2021). Other types include Bandwise regression: a specific case of stepwise multiple regression (SWL) in which the explanatory variables are measures of reflected energy in sensor-specific spectral bands (Porter et al., 2014; Lawrence et al., 1998). New powerful approaches also include combining regression analysis and machine learning techniques.

3. AIM OF THE STUDY

The aim of the study is to evaluate the correlation between grassland DM production and remote sense data, and to investigate the remote sense data potential in estimating AGB of grasslands, analyzing different aspects of a pasture located in a mountain area. The study was conducted comparing field-based and satellite measurements. This research intends to evaluate the relationships between vegetation indices and DM production, and how the use of high-resolution satellite data and geospatial analysis techniques can enhance the ability to monitor and manage mountain grasslands, providing valuable information for agricultural production, conservation efforts, and habitat management. Indeed, improved biomass estimation supports efficient grazing strategies. Hence, it contributes to broader ecological and socio-economic objectives, such as climate change mitigation, biodiversity protection, sustainable land use and food security.

4. MATERIALS AND METHODS

4.1 Research Area

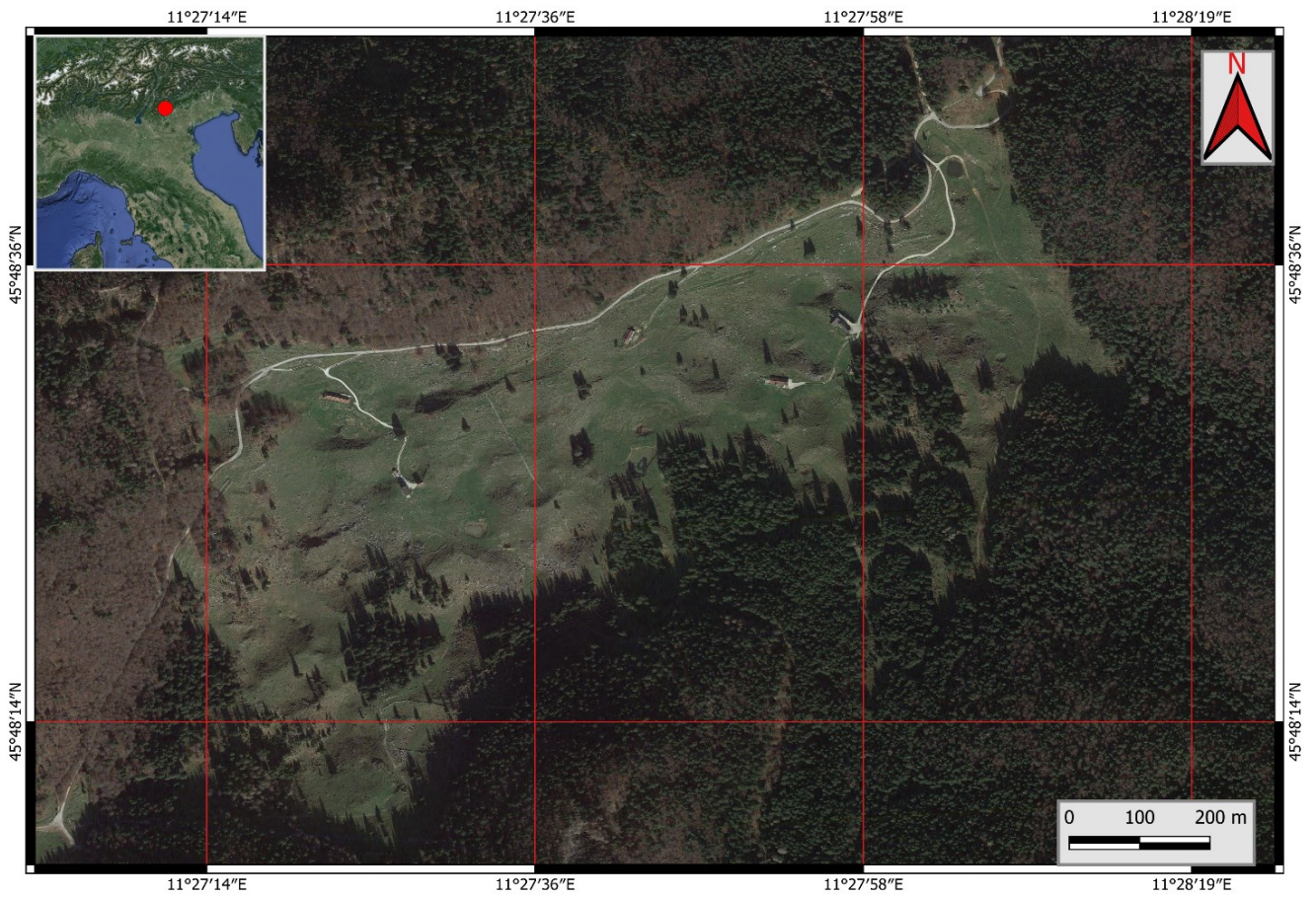


[Figure 1. QGIS top view of the research area]

The study was conducted at Malga Carriola, located in Caltrano within the Vicenza Province (45°48' N, 11° 46' E, altitude 1240 m above sea level) and 8 km away from the Asiago Plateau (Figure 1).



[Figure 2. Side view of Malga Carriola]

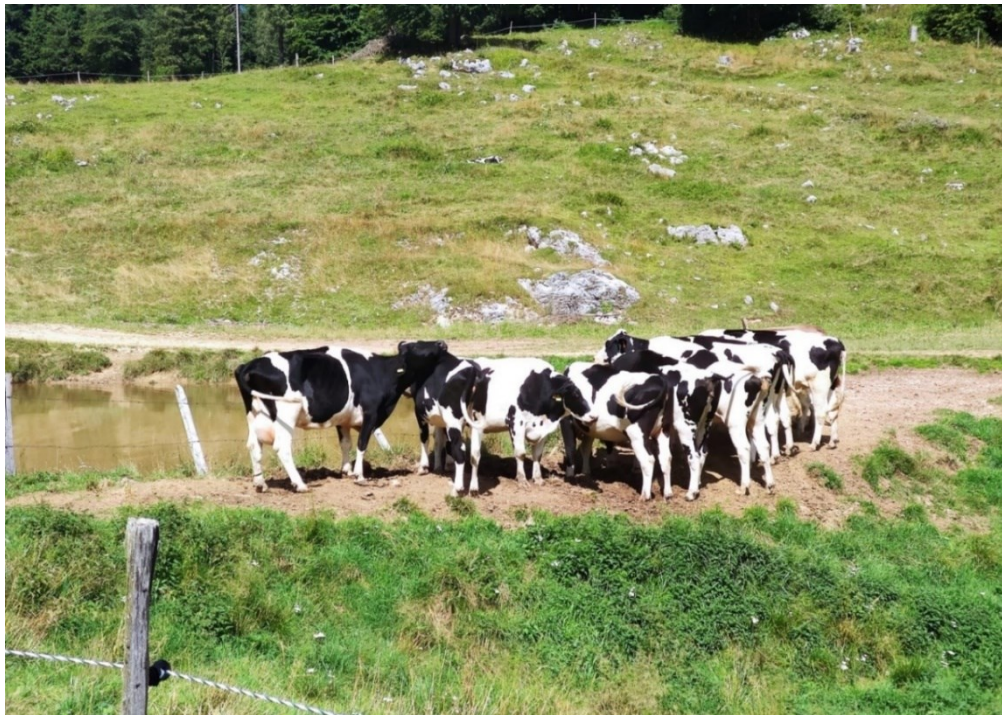


[Figure 3. Holstein Friesian cows grazing]

Malga

“Malga” (or Alpe) is the Italian term used to refer to temporary agro-zootechnical activities carried on alpine grasslands. They are active for a limited period of the year, normally from 90 to 120 days, and include a wide set of fixed and mobile factors (land, buildings, paddocks, livestock, tools). They form true agricultural communities, representing unique human adaptation to mountain areas. These settlements are common in the alpine regions of Europe, such as Italy, France, Austria, Germany, Liechtenstein, and Slovenia. In Italy, they can be typically found between 600 m and 2500 m above sea level. The activities consist of bringing animals to the mountain pasture (transhumance), starting with the “montication” (mountain climbing) between the end of May and mid-June, and ending in late September with the “demontication” (descent back to the low-altitude areas).

Cows can graze in ideal and natural environments, feeding on fodder rich in varieties that provide high nutrient values, medicinal properties, and aromatic substances that give milk and cheese special fragrances. Livestock’s daily movement in these wide areas promotes muscle development, improving strength and blood circulation, resulting in stronger animals. Furthermore, at higher altitudes, the better air quality and the intense active radiation (higher UV light quantity) have beneficial effects on their health.

The agricultural alpine economy is strictly linked to the agricultural activities carried out in the valley. Indeed, while in summer, the low-altitude fields and meadows are used for the production of fodder (to be used during cold seasons), the livestock is brought to the high-altitude grasslands. In the past, goats and sheep were commonly employed, while nowadays there are mostly cows. However, some “mixed” malghe settlements with cows, goats, sheep, or horses still exist. Malghe can have different organizational and management systems (i.e., public-owned, private, rented). Public ones are often influenced by strict leasing contracts to tenants and other public management agreements.

Historically, malghe have been organized to integrate various components, both fixed and mobile. In addition to lands, paddocks and grazing units for livestock, they also include spaces for milk processing, cheese aging, as well as housing structures for personnel and tourists.

Overtime, the aims and techniques for utilizing malghe have changed as the societal needs keep transforming. Up to few years ago, their activities were totally oriented to traditional and local agricultural production, such milk, cheese, meat, and forage. Nowadays, instead, they also include touristic and educational activities, while preserving the natural and cultural heritage of the place.

One of the principal challenges for malga managers is to optimize forage consumption by animals, also considering the nutritional quality and palatability of available grass. At the same time, it is essential to preserve the value of the pasture throughout the season, avoiding weed proliferation and minimizing geological events (i.e erosion) that could compromise animals' productivity and the environmental services.

4.2 Soil features

Caltrano area exhibits undulating summit surfaces and uniformly inclined tabular reliefs of the Pre-Alps (Southern Alps). Within this area, soil profiles range from poorly calcareous to moderately calcareous, consisting mainly of thickly stratified hard limestones and marly limestones derived from the Jurassic-Cretaceous stratigraphic series.

Both parent material and substrate are composed of limestone rock. Sub-flat to undulating surfaces and slopes are locally affected by karst phenomena of various scales (i.e. dry valleys, sinkholes). The permeability of these soils is moderately high, facilitating moderately rapid to rapid internal drainage processes. Depending on the specific location, surface stoniness contains gravel (1-5% range) and pebbles (1-2%). The rockiness level is moderate (1-3%). Figure 3 and Figure 4 show the soil composition detail for Veneto region and Vicenza province respectively. This data is available on the *Agenzia Regionale per la Prevenzione e Protezione Ambientale del Veneto* (ARPAV) website.

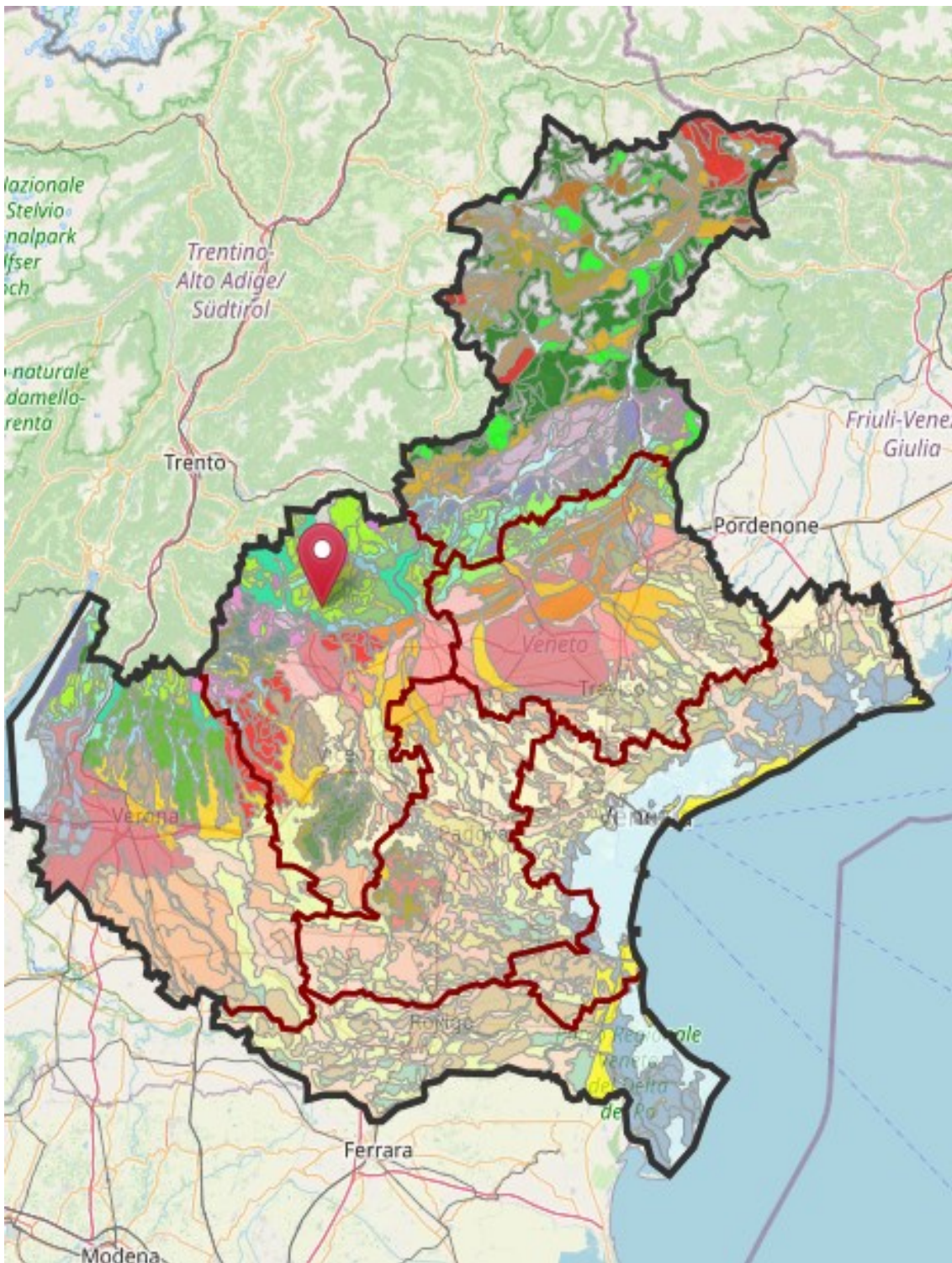


[Figure 3. Soil map of Veneto region. Source: ARPAV]

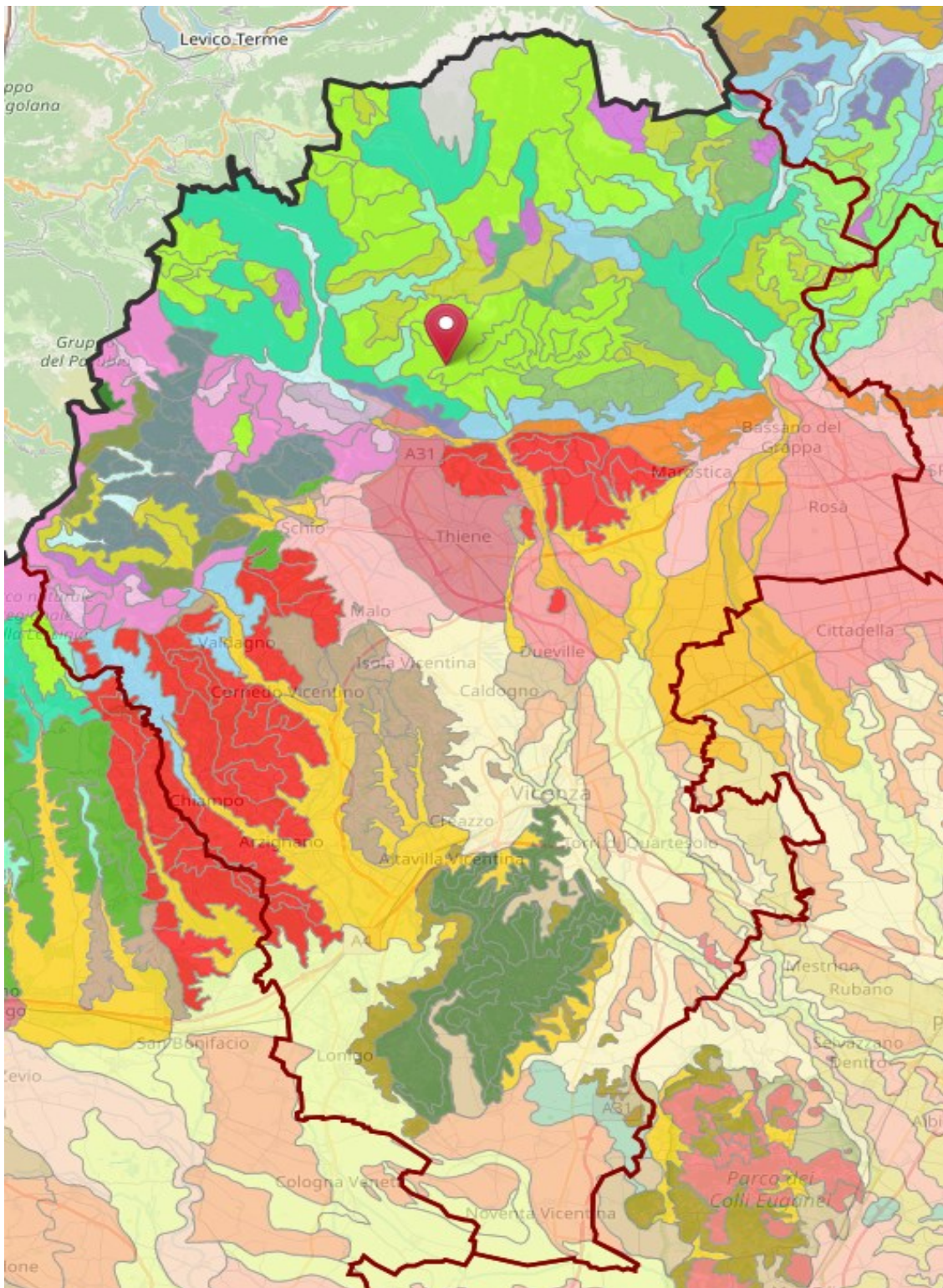
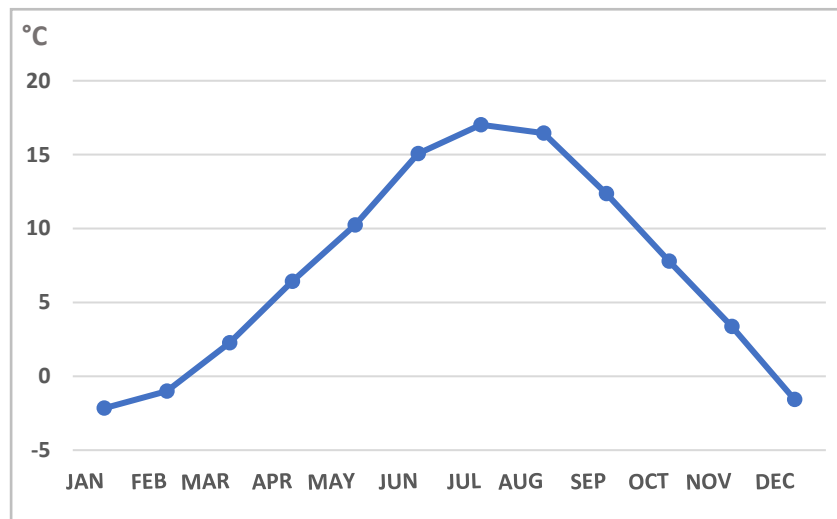


[Figure 4. Soil map of Vicenza province. Source: ARPAV]

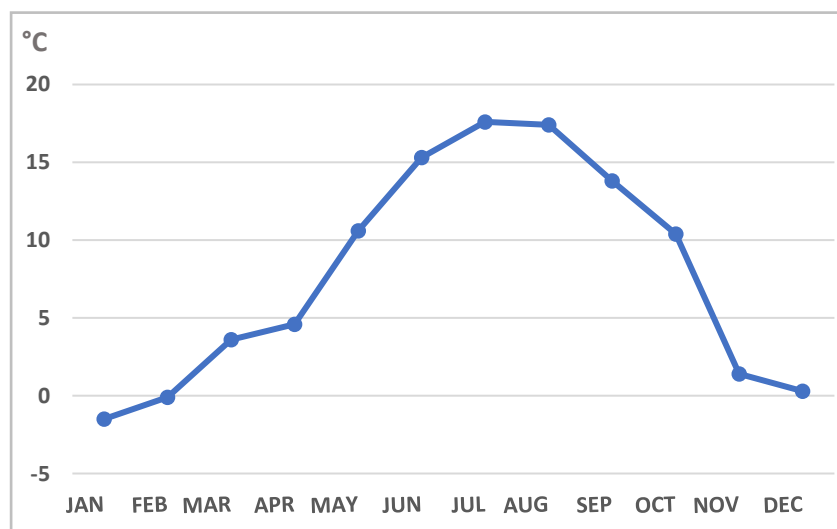
4.3 Climate data

Veneto region is characterized by different climate zones: lowlands, prealpine and alpine zones. The study area of Malga Carriola in Caltrano (Vicenza) falls under the prealpine climate zone, where abundant precipitations are usually recorded, with average values of 1200-1500 mm/year and up to 2000 mm. Twelve Celsius degrees is the average temperature value in this zone, and it is not so different from the average values registered in lowlands (Salvan et al., 2023; Basso et al., 2020). The climate data was acquired from the meteorological station of Asiago Airport, available on the *Agenzia Regionale per la Prevenzione e Protezione Ambientale del Veneto* (ARPAV) website.

Temperature



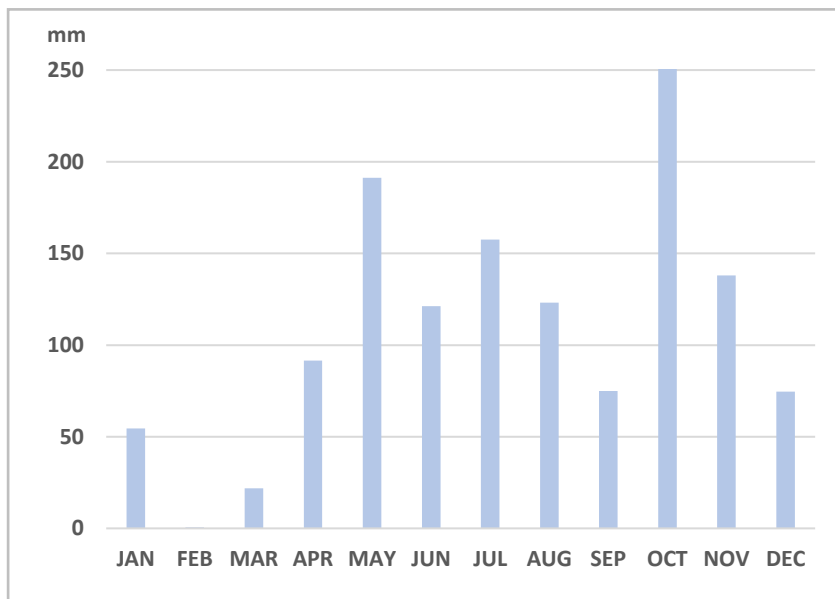
[Figure 5. Mean temperature 2023]



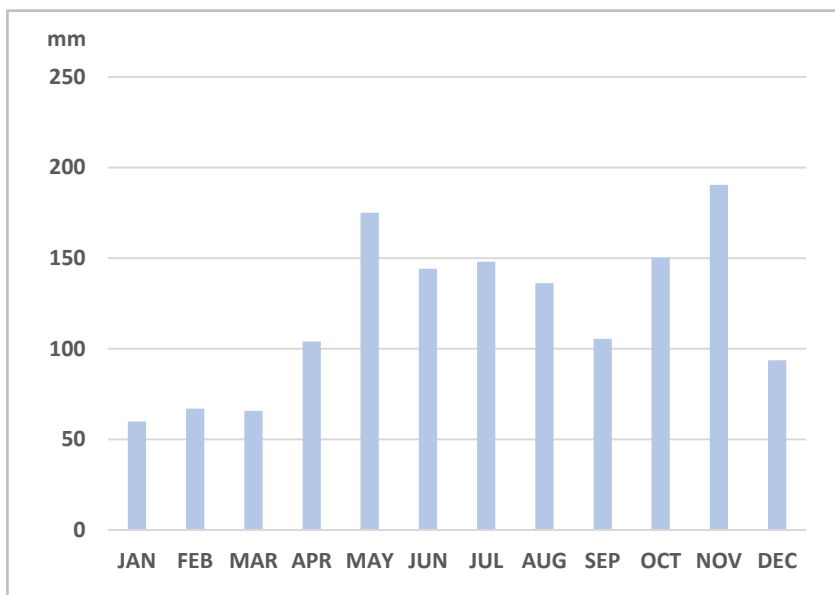
[Figure 6. Mean temperature 2010-2022]

Figure 5 presents the mean temperature data for the year 2023. Within this period, the minimum recorded mean temperature was -1.7°C and the maximum mean temperature was $+17.4^{\circ}\text{C}$. Figure 6 illustrates a broader temporal perspective by showcasing the mean temperature trends for the multiyear period 2010-2022.

Precipitation



[Figure 7. Rainfall distribution 2023]



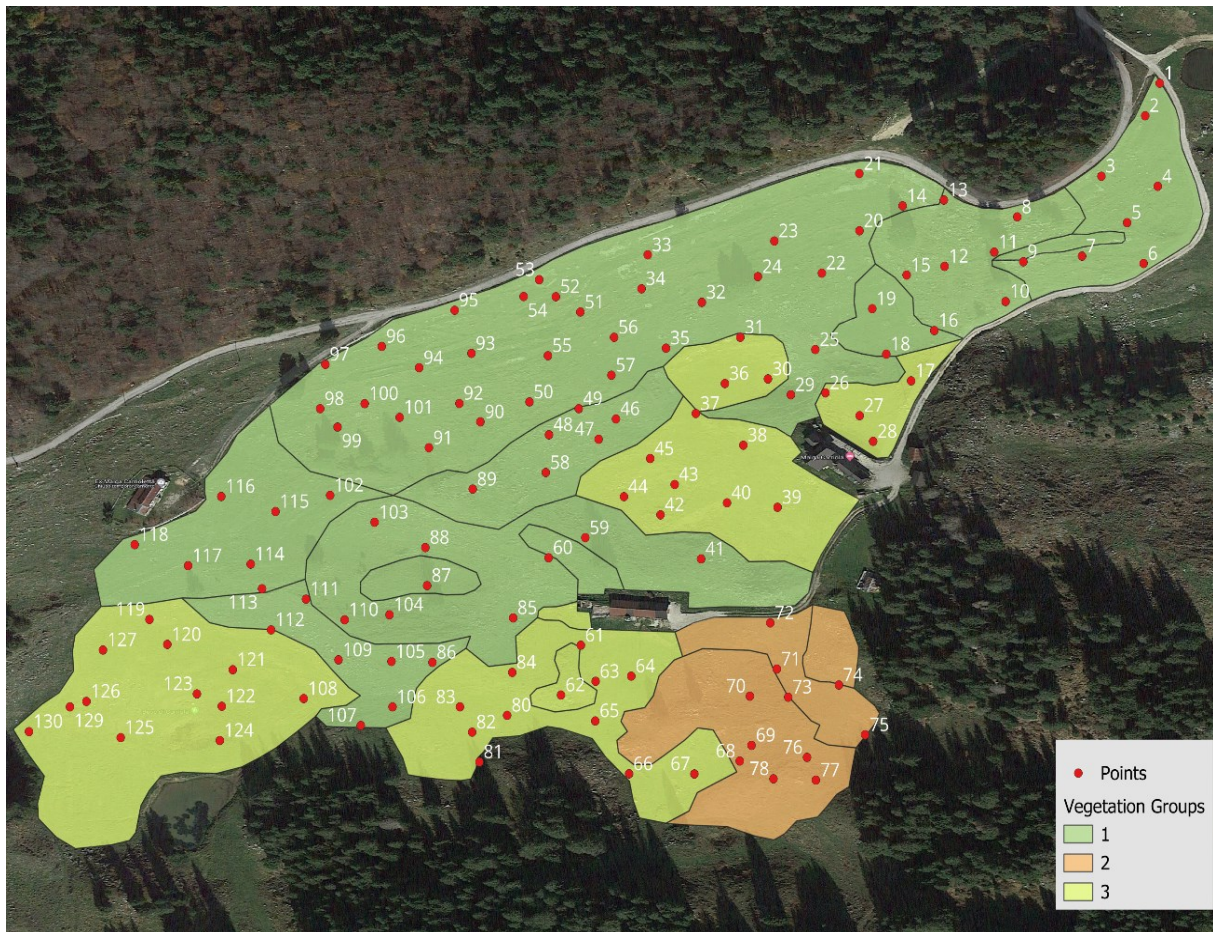
[Figure 8. Rainfall distribution 2010-2022]

Figure 7 illustrates the rainfall distribution for 2023, year in which 1339 mm of rainfall was recorded. Figure 8 shows the mean precipitation trend for the multiyear period 2010-2022.

4.4 Data collection and analysis

Ground-field measurements

The experiment was conducted over a period of five months (July – October) in 2023. Twenty-three botanical surveys were conducted recording all plant species and their abundance, to draw a vegetation map of the grazing surface.



[Figure 9. Vegetation map and ground-field measurement points on QGIS]

Figure 9 shows the vegetation map composed of three groups representing the most abundant species. Group 1 (green): vegetation dominated by *Festuca rubra*, with secondary species such as *Centaurea jacea* and *Phleum pratense*; Group 2 (yellow): vegetation dominated by *Trifolium repens* and *Trollius europaeus*, with auxiliary species like *Trifolium pratense* and *Phleum pratense*; Group 3 (orange): vegetation mainly characterized by the presence of *Brachypodium caespitosum* and *Rhinanthus*.

A random selection of 130 points was performed over the grazing surface using QGIS. The software was used to delimit the study area and identify 130 points. The research area was divided into several polygons, which were later sorted by their features into three groups corresponding to the three identified pasture vegetation categories. At each point the vegetation height measurement (Rising Plate Meter, Grasshopper) and a forage sample in tasted areas of 1 m² (handheld grass trimmer) were collected in July 2023. The forage samples were dried in ovens at 105°C for 36 hours and subsequently weighed to assess the amount of dry matter (DM).

Remote data

Considering the small area of Malga Carriola and the need for a high spatial resolution, images from Sentinel-2 with a 10 meter resolution were selected. In Google Earth Engine (GEE)'s platform toolset, a specific Java Script code was inputted to obtain raster imagery of the research location, with a specific focus on the temporal span from March to November, and NDVI (Normalized Difference Vegetation Index) and NDTI (Normalized Difference Thermal Index) as vegetation indices particularly interesting for the aim of this research. Google Earth Engine is a cloud-based geospatial analysis platform that provides data and satellite images for academic, non-profit, business and government users. After recording these VIs during the study period, only some values for specific dates were chosen for the purpose of this research. The date selection was based on two criteria: a) relevant NDVI/NDTI values (> 0,3); b) values recorded under favorable atmospheric conditions to avoid nuisance caused by clouds.

The selected dates were:

- March: 9, 29
- May: 23
- June: 17
- July: 7, 23, 27
- August: 6, 11, 16, 21, 31
- September: 10, 25, 30
- November: 23, 29

NDVI was selected for its proven effectiveness, by extensive research over many years, in tracking changes in vegetation density and cover, as well as vegetation health. NDTI was chosen for its significant capacity to detect areas with little to no vegetation cover, indicating bare soil and/or the presence of rocky material. Moreover, there was a need for further research and evidence to unlock its potential in AGB estimation and, more in general, grassland protection studies. Raster datasets from Sentinel-2 were imported to have a full visualization of the VIs trends, also facilitating the creation of points attribute tables (including VIs at different dates, vegetation height, DM, and slope) for further data analysis. Digital Elevation Models (DEMs) of the slopes were downloaded from the geoportal of Veneto Region. Excel was used to process the QGIS attribute tables for data visualization of NDVI and NDTI trends over the research period.

Statistical Analysis

According to the vegetation map, a code corresponding to a vegetation type was assigned to each point (from 1 to 3). Dry matter and vegetation height were correlated with remote sensing data (NDVI and NDTI) acquired on July 12th, and July 17th, with the mean of the two dates, and with the slope of each point. The choice of the two specific dates was based on overlapping ground-field and satellite flights dates, allowing for separate analysis of the two days of July, followed by averaging to remove any disturbances due to the weather conditions. July was also selected as it corresponds to a stage of steady vegetative growth, thus it marks the midpoint of the study period. The matrices of data resulted from NDVI and NDTI series were subjected to hierarchical cluster analysis. According to cluster analysis grouping of both NDVI and NDTI series, a code corresponding to a group (from 1 to 4) was assigned to each point. Furthermore, generalized linear models (GLMs) were built to explain observed variation in measured parameters (vegetation height, DM, slope) depending on groups obtained with cluster analyses (vegetation type, NDVI and NDTI). Full GLMs, including group classifications, were simplified based on Akaike's Information Criterion (AIC). Significances were determined by likelihood-ratio tests (LRT) of reduced versus full models. ANOVA was performed to determine whether the groups created through cluster analysis (NDVI, NDTI, Vegetation) were influenced by Grass Height, Grass Dry Matter and Slope. All statistical analysis were performed using R project (R core teams, 2023).

5. RESULTS AND DISCUSSION

5.1 Correlation Analysis

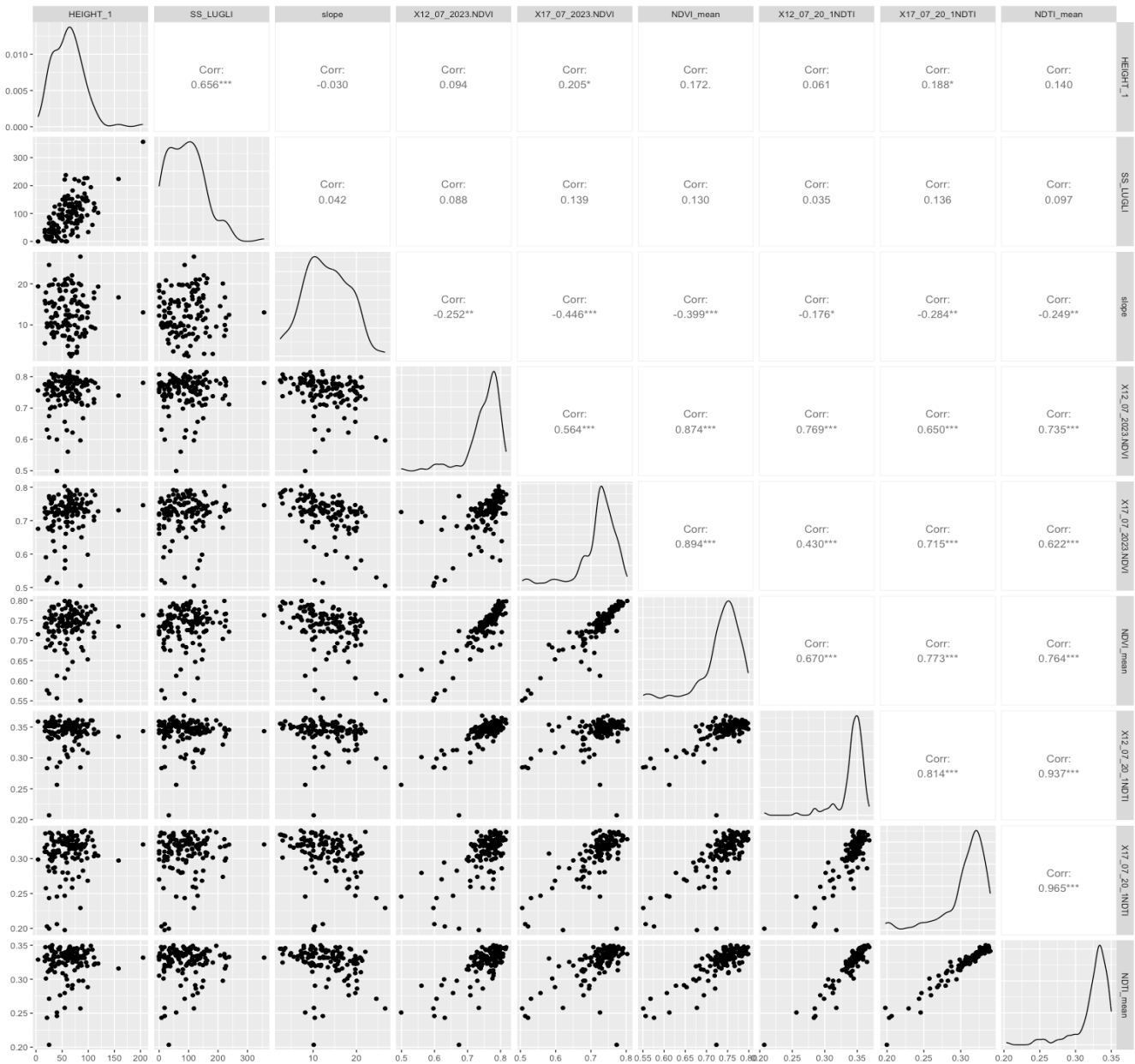


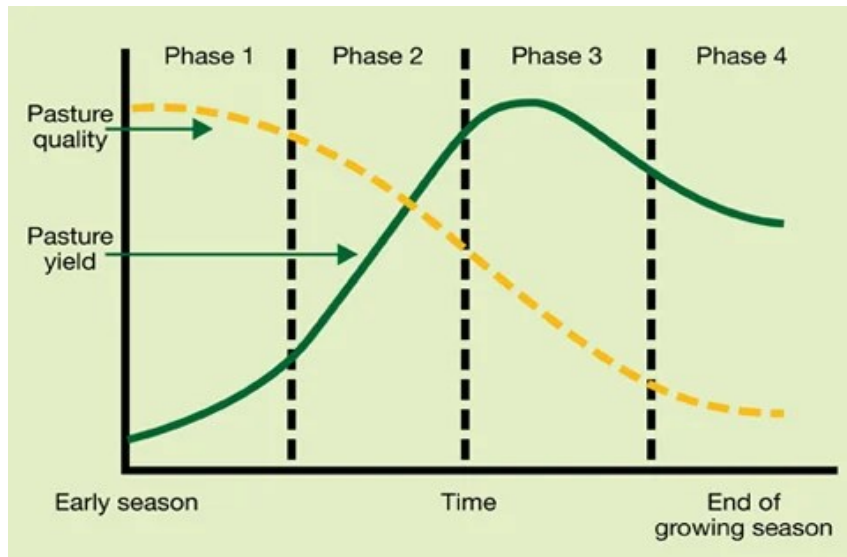
[Figure 10. Correlation matrix illustrates the results, organized into scatter plots, density plots and correlation values. Outcomes are classified as (***) strong correlation, (**) moderate correlation, and (*) weak correlation]

The main results emerging from the correlation analysis were:

- 1) Overall strong positive correlation between Grass Dry matter and Grass Height (0.656***). The relative scatter plot shows points arranged very close to each other, forming an upward diagonal. This indicates a direct relationship between the two variables, as grass height increase shows a proportional increase in dry matter content.
- 2) Weak positive correlation between NDVI and Grass Height (0.205*) on July 17th. The points in the scatter plot show a wider arrangement with a slight upward trend, meaning that NDVI is poorly affected by the increase in grass height and indicate little role in determining its values.
- 3) Moderate negative correlation between NDVI and Slope (-0.252**) on July 12th. Close points form a downward pattern in the scatter plot. This shows an indirect relationship between the variables, suggesting that NDVI tends to decrease moderately as slope increases.
- 4) Strong negative correlation between NDVI and Slope (-0.446***) on July 17th. The points manifest a clear downward distribution. As slope increases, NDVI values decrease proportionally.
- 5) Strong negative correlation between NDVI mean values and Slope (-0.399***). This confirms that regions with steep slopes show low NDVI values, impacting on either vegetation presence or vegetation health, as illustrated by the evident downward pattern of the points.
- 6) Weak negative correlation between NDTI and Slope (-0.176*) on July 12th. The points have a wider arrangement with a slight downward trend, suggesting that NDTI tends to decrease slightly as slope increases.
- 7) Weak negative correlation between NDTI and Slope (-0.284*) on July 17th. Same point distribution. NDTI value trends are also proven for this date.
- 8) Moderate negative correlation between NDTI mean values and Slope (-0.249**) Same point distribution. These results confirm the existence of an inverse relationship between NDTI and slopes.

5.2 Pasture growth trends

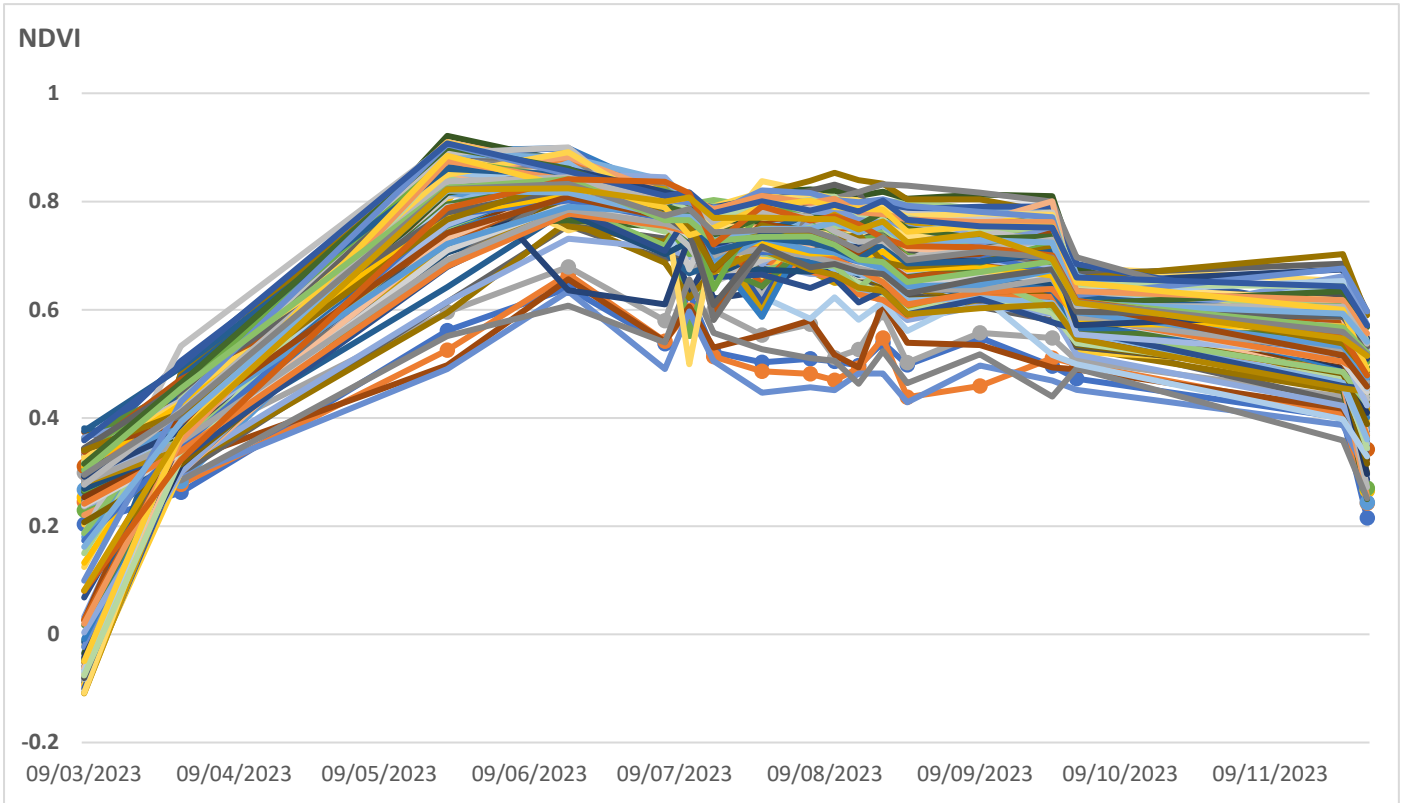
Mountain pastures are mainly composed of herbaceous species (or grass), whose growth follow specific patterns: a sigmoidal curve characterized by an initial increase, followed by a “plateau” and a decline (Figure 11). Grass undergoes two main stages: vegetative and reproductive.



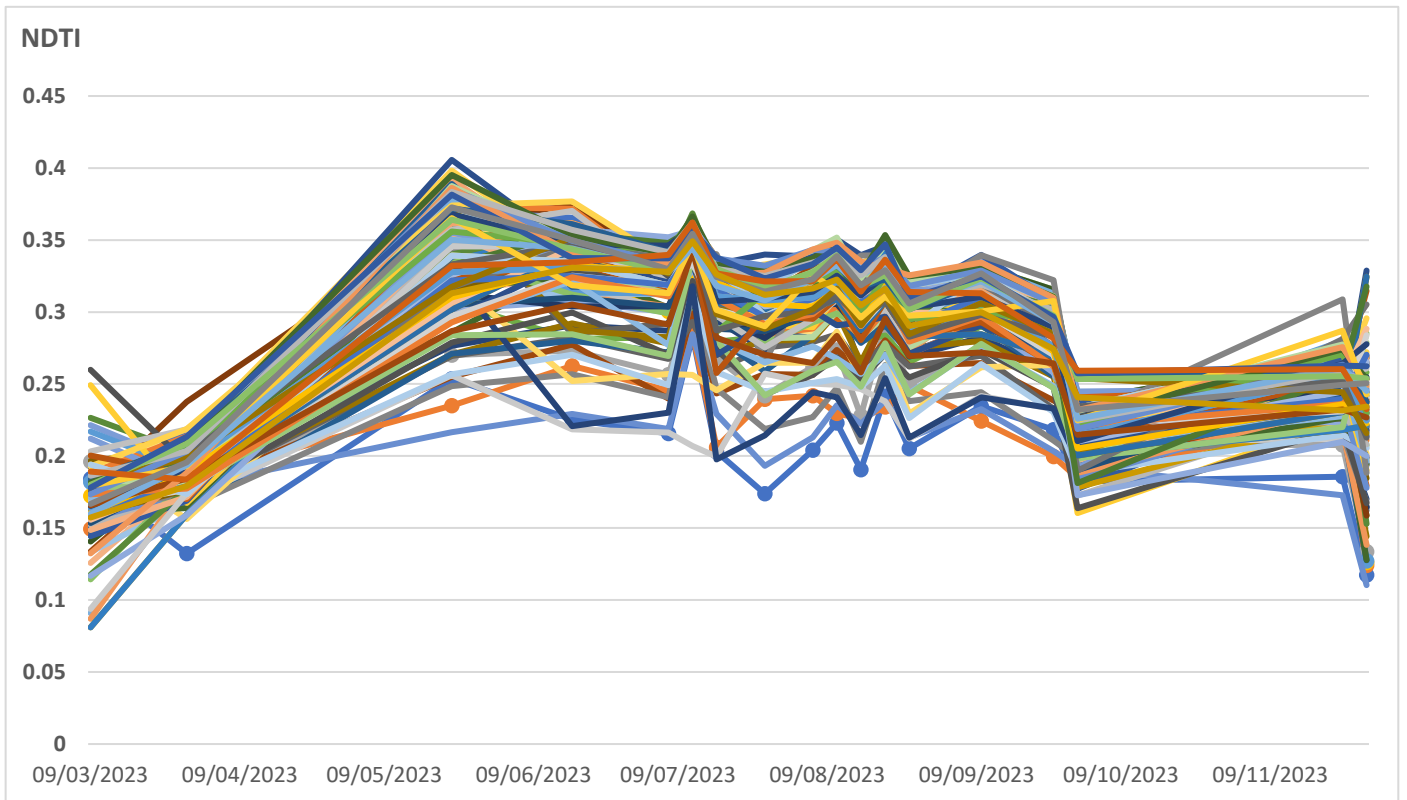
[Figure 11. Plant growth trend. Source: www.mla.com]

During the early vegetative season, plants are slow growing (Phase 1), as they haven't developed enough leaf area to produce energy through the photosynthesis. In this stage, plants rely on nutrients stored in the crown and roots to support leaf and structure development. Pasture quality is at its highest, as their leaves are highly digestible, and rich in protein and energy, but this is also a phase in which repeated grazing and/or heavy machine tillage activities can deplete the nutrient reserves, reducing vigor, productivity and overall vegetation health. In Phase 2 plants grow rapidly, as they have established enough leaf area, utilizing efficiently the sunlight for producing energy. Pasture quality is also high during this stage, with high levels of biomass and great digestibility. Once grass enters the reproductive stage (late Phase 3 and Phase 4), it begins to lignify and produce elongated stems that will support a seedhead. Pasture yield (biomass) reaches the peak during this period and starts its decreasing trend. Pasture quality is critically reduced, and in the last stage (Phase 4), leaves become shaded and die, resulting in lower yields, lower nutrient concentrations and digestibility (Alford A. et al., 2003).

5.3 VIs seasonal trends



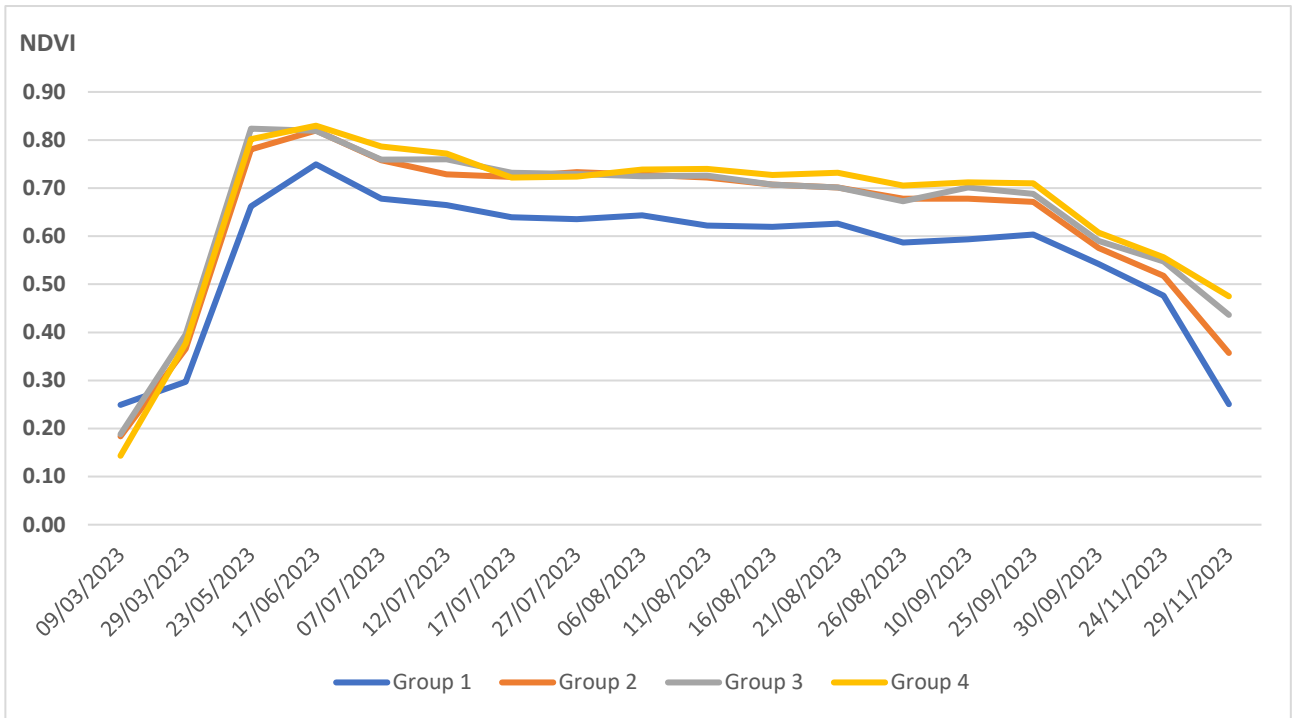
[Figure 12. NDVI points trends throughout the season]



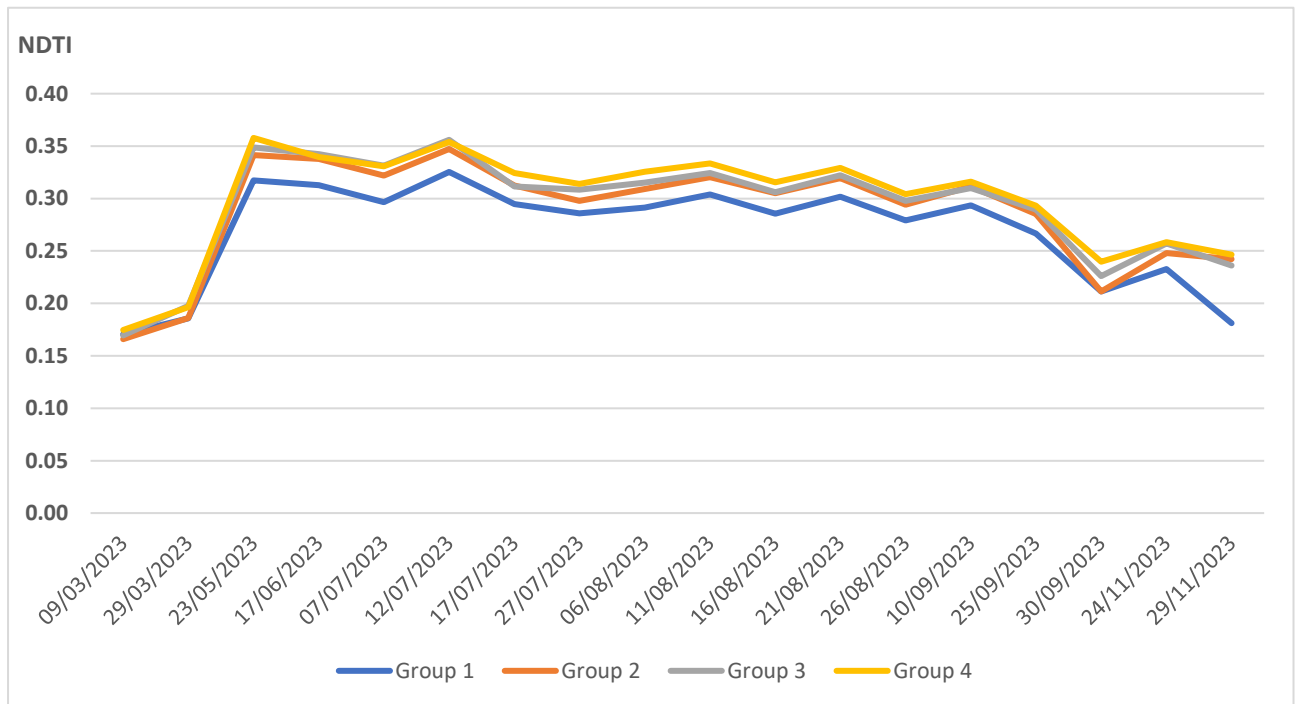
[Figure 13. NDTI points trends throughout the season]

Figure 11 and Figure 12 show the progression of the 130 points during the research period for the chosen VIs. Points for NDVI and NDTI clearly reflect the typical vegetation growth patterns, also showing other behaviors: initial increase, peak, post-peak fluctuations, stabilization and final decrease. Points manifest a notable increase from March to May, suggesting an active vegetation growth and favorable thermal conditions. For both VIs, the peak is reached on the same date: 25th May. Post-peak values from May to September display different fluctuation trends, concerning primarily NDTI. For the latter, the continuous variation – with two other minor peaks on 12th July and 28th August – suggests that thermal conditions keep changing, possibly affecting plant water stress and soil moisture content. On the contrary, NDVI exhibits less variability in the same time span, meaning that grass has reached a stable growth stage. These differences highlight the sensitivity of the indices to different factors: NDVI is more stable as it follows the vegetation growth dynamics, while NDTI is more sensitive to thermal changes occurring throughout the season.

As approaching the end of the growing season (September-November) both NDVI and NDTI point trends show the same drop on 30th September, followed by steady trends and a final decrease in late November, reflecting the arrival of colder temperatures and a reduced vegetative activity. Overall, although many of the points show similar behaviors during the research period, many others follow other trends. For this reason, it was deemed necessary to provide further insights on their similarities through additional analysis.



[Figure 15. NDVI groups mean values]



[Figure 16. NDTI groups mean values]

Figure 16 and Figure 17 respectively show the trends of the four NDVI and NDTI groups derived from the cluster analysis during the research period.



[Figure 17. NDVI groups distribution on map]

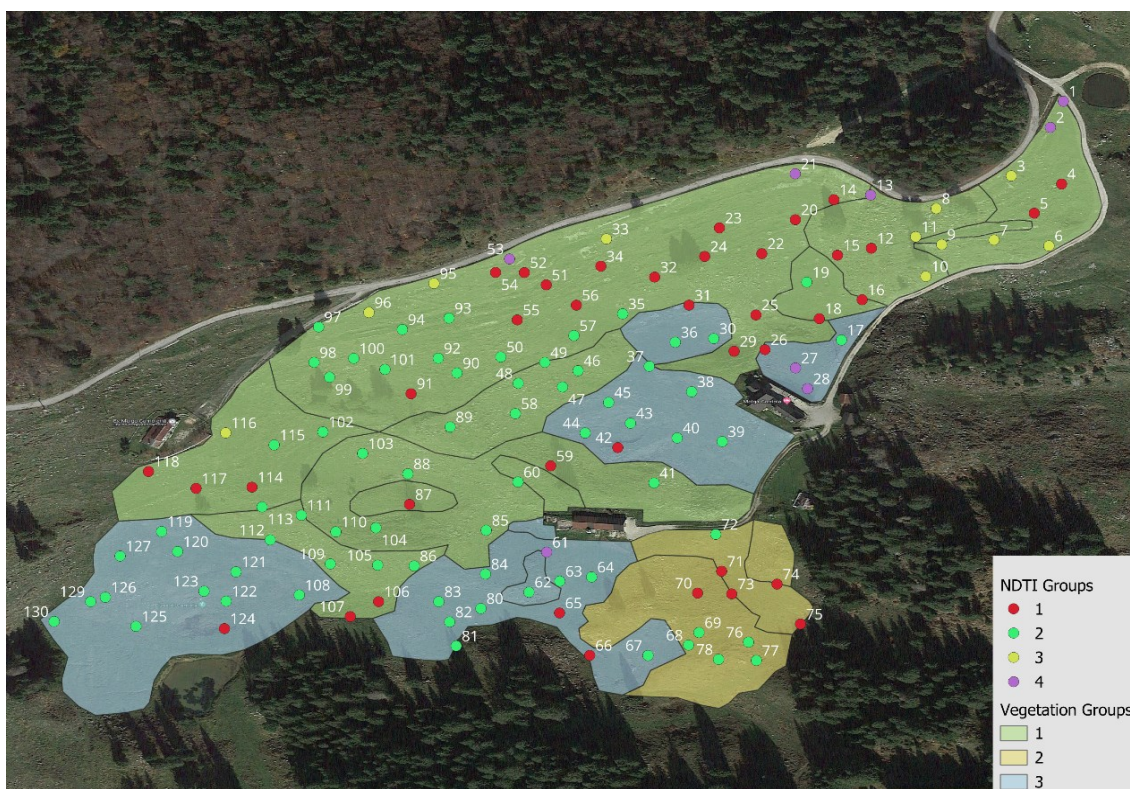


[Figure 18. NDTI groups distribution on map]

Figures 17 and 18 show how the 130 points are distributed on the vegetation map, with details on the four groups determined by the cluster analysis, both for NDVI and NDTI. As illustrated, no direct relationships between the two VIs can be found in the distribution of the points. Group 1 (red) is distributed only in the upper-right edge of the map for NDVI, while it is more dispersed in the NDTI map. For NDVI, Group 2 (green) appears to be more concentrated in specific zones, whereas for NDTI it is widely spread. For both VIs, Group 3 (yellow) points are clustered in the upper-right quadrant of the map. Finally, Group 4 (purple) is mainly located in the central part of the map for NDVI, while it is dispersed along the top-right edge of the map for NDTI. Better evidence can be found if considering the relationship with vegetation. Normalized difference vegetation index groups appear to be related to the Vegetation Groups (i.e. Group 4 NDVI with Group 1 Vegetation, Group 2 NDVI with Group 3 Vegetation). On the contrary, NDTI Groups show a more scattered and varied distribution. In general, NDVI appears to have a correlation with vegetation, while NDTI does not, suggesting that it can be influenced by other factors not directly related to vegetation.

5.5 Analysis of variance (ANOVA)

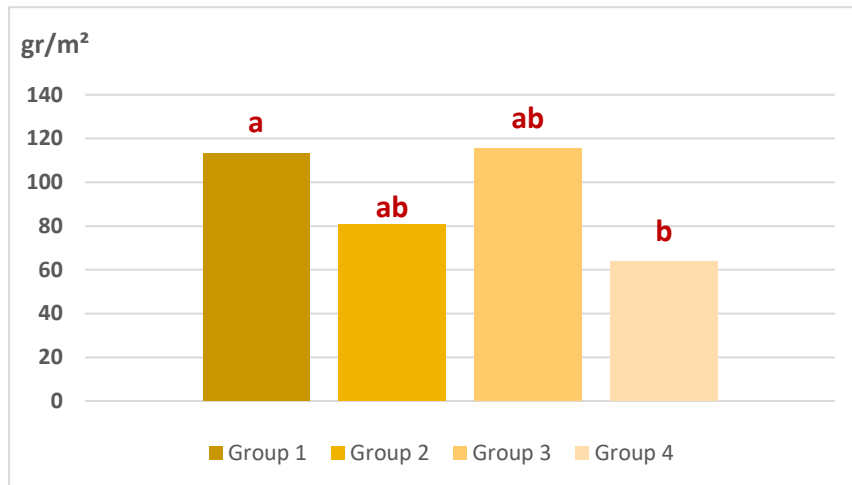
Figure 19 exhibits the results of ANOVA carried out for NDVI, NDTI and vegetation groups.

	NDVI Groups	NDTI Groups	Vegetation Groups
Grass Height	ns	ns	ns
Grass Dry Matter	ns	*	ns
Slope	***	**	***

[Figure 19. ANOVA table results, * significant at $p < 0.05$; ** significant at $p < 0.01$; *** significant at $p < 0.001$; ns, no significant]

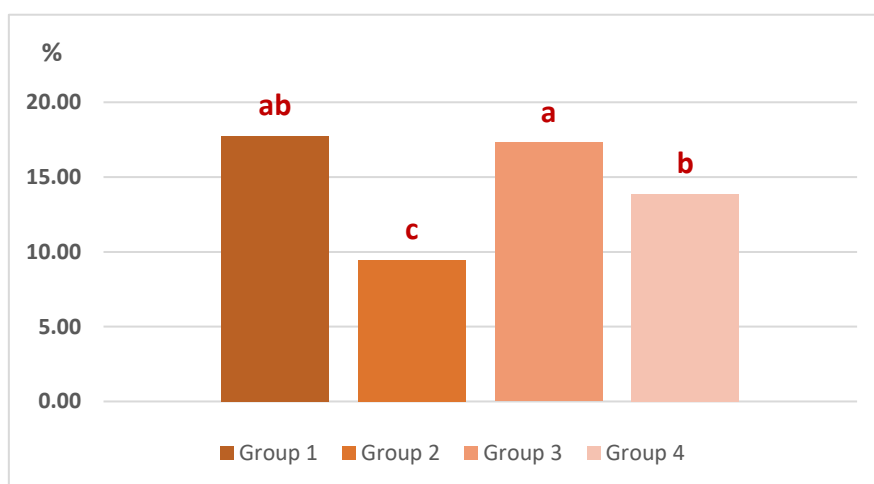
The ANOVA indicated that NDVI, NDTI, and vegetation groups were significantly affected by slope, while grass dry matter affected only NDVI. All three groups were not significantly affected by grass height. Since ANOVA only suggests the presence of differences among the elements of study, further analysis such as *post-hoc* test was needed to determine which specific groups are different from one another.

Figure 20 shows the results of *post-hoc* test performed to determine the relationship between the four NTDI groups derived from cluster analysis and Grass Dry Matter, using average values. Group 1 is not different from Group 2 and 3, while it is significantly different from Group 4; Group 2 and 3 are not significantly different from each other and from Group 4.



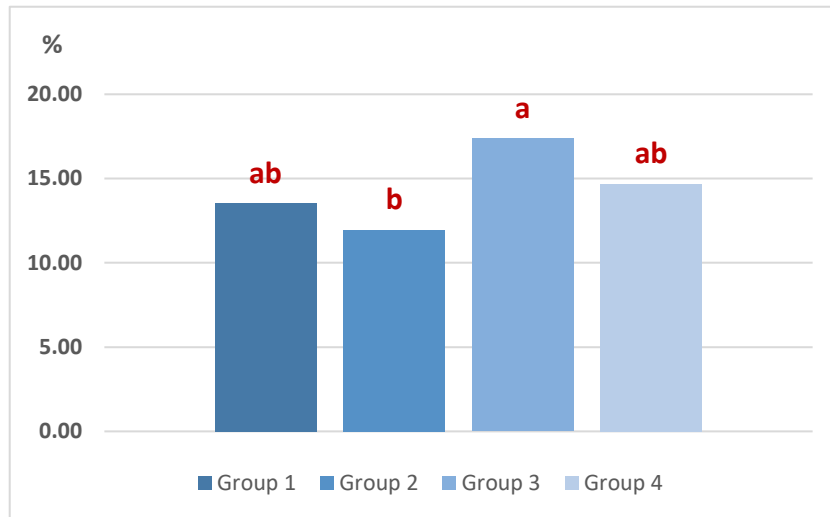
[Figure 20. NTDI-Dry Matter *post-hoc* results, bars with the same letters are not significantly different from one another (P<0.05)]

Figure 21 illustrates the outcomes of *post-hoc* test performed for the relationship NDVI-Slope. Group 1 is not significantly different from Group 3 and 4; Group 2 is significantly different from Group 1, 3 and 4, while Group 4 significantly differs from Group 2 and 3.



[Figure 21. NDVI-Slope *post-hoc* results, bars with the same letters are not significantly different from one another (P<0.05)]

Post-hoc test results for NDTI-Slope relationships are showed in Figure 22. Group 2 is significantly different from Group 3, but not significantly different from Group 1 and 4. Group 3 and 4 are not significantly different from each other, nor from Group 1.



[Figure 22. NDTI-Slope *post-hoc* results, bars with the same letters are not significantly different from one another ($P<0.05$)]]

Figure 23 shows the results for the relationship between the three Vegetation groups and Slope. Group 1 and Group 2 are not significantly different, while Group 3 is significantly different from Group 1 and Group 2.

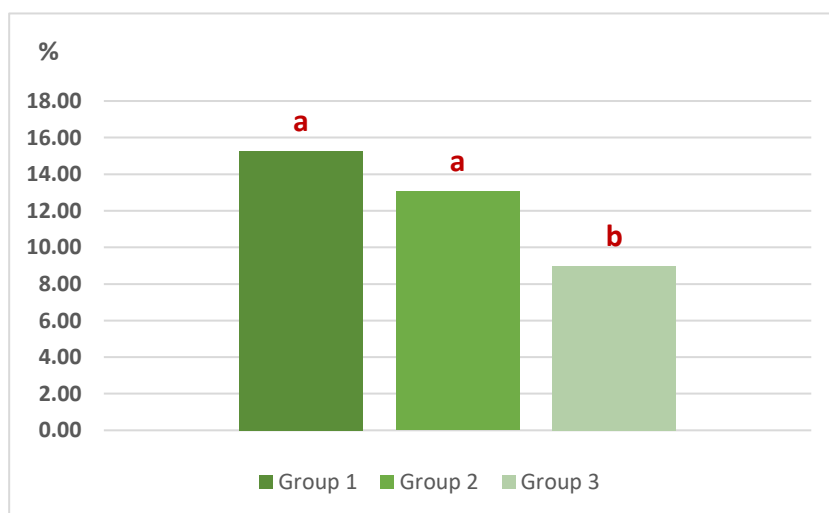


[Figure 23. Vegetation-Slope *post-hoc* results, bars with the same letters are not significantly different from one another ($P<0.05$)]]

Main understandings from ANOVA

In the study period selected, NDVI appears to be able to differentiate between steeper and less steep areas, with no significant capacity in detecting any other effects on grass productivity (dry matter) and/or grass height. Despite showing similar results, NDTI goes further and provides more information about the relationship with dry matters, as a weak significance has emerged from ANOVA. Vegetation, just like NDVI, only gives information on slopes.

6. CONCLUSIONS

Despite previous research indicating a relationship between VIs and DM production, this study did not show any significant correlation. NDVI and NDTI data allowed to identify four groups of points manifesting different trends. Mapping these trends revealed a non-strong correspondence between VIs and vegetation. In particular, NDVI has showed not be a robust predictor of neither Grass Height nor Grass Dry Matter, suggesting its inaccuracy in estimating AGB in such conditions. Nonetheless, NDVI's moderate to strong negative correlation to Slope marks the fact that, on steeper slopes, vegetation is less dense and/or healthy, emphasizing the importance of considering topography for this kind of assessments.

Although it has a weak correlation with Slope, on the other hand, NDTI gave better results. In fact, the stable negative correlation trends over time, show how NDTI can be reliable in reflecting the changes in vegetation related to the slope. Hence, the sensitivity to soil and vegetation thermal conditions makes NDTI a valuable complementary index to NDVI, especially in different topographic situations.

In conclusion, this study demonstrates the complexity of using NDVI and NDTI for AGB estimation in alpine pastures characterized by great heterogeneity, suggesting that other factors can be involved in determining vegetation production and distribution. However, an accurate biomass estimation should include long-term monitoring and all plant growth stages, as spectral data vary with biomass allocation in different plant organs. Moreover, integration of additional variables, testing multiple remote sensing platforms, and utilizing multiple VIs, can be important for defining accurate vegetation assessments, resulting in enhanced grassland protection activities.

ADDITIONAL MATERIAL

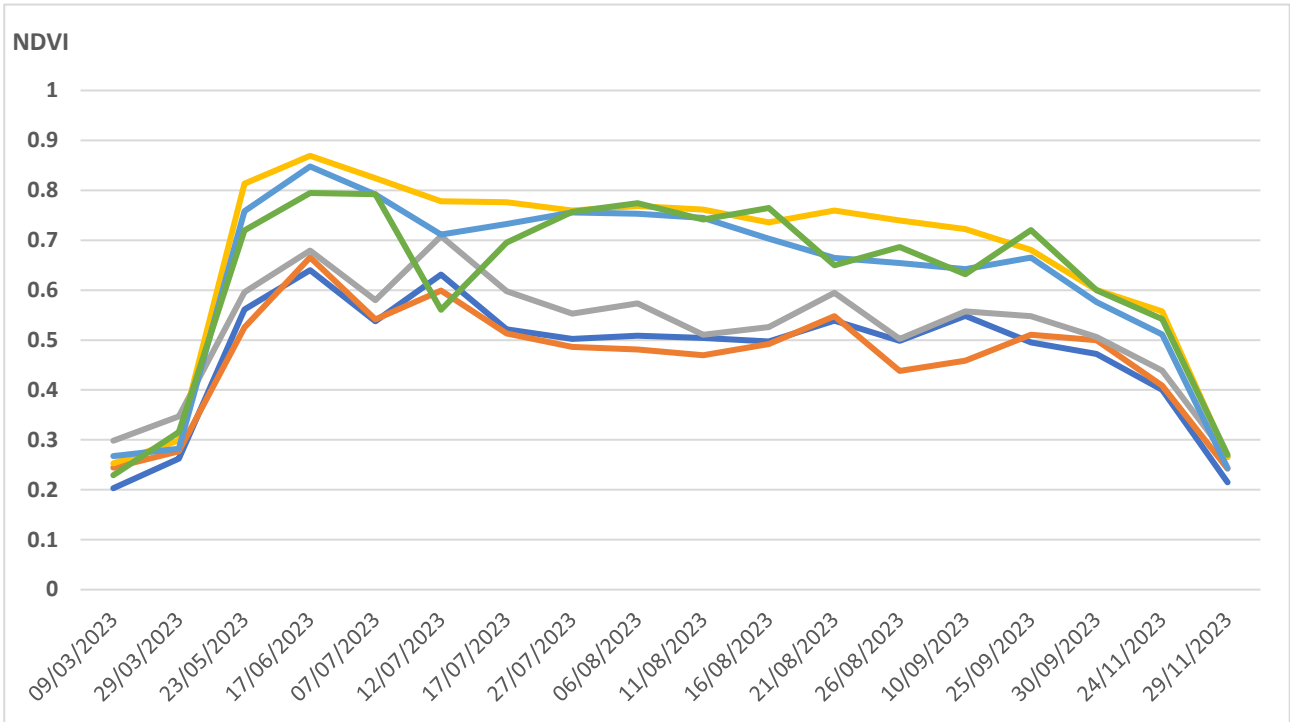


[Figure 24. NDVI Group 1 trend derived from cluster analysis]

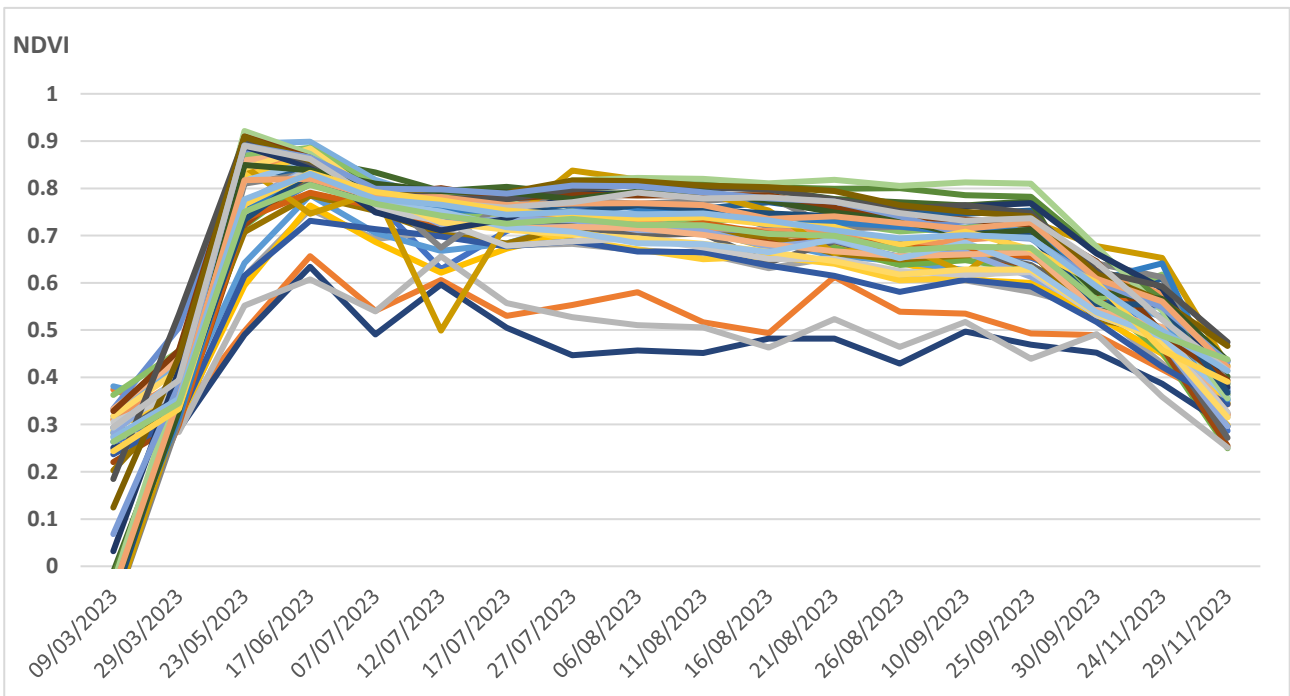


[Figure 25. NDVI Group 2 trend derived from cluster analysis]

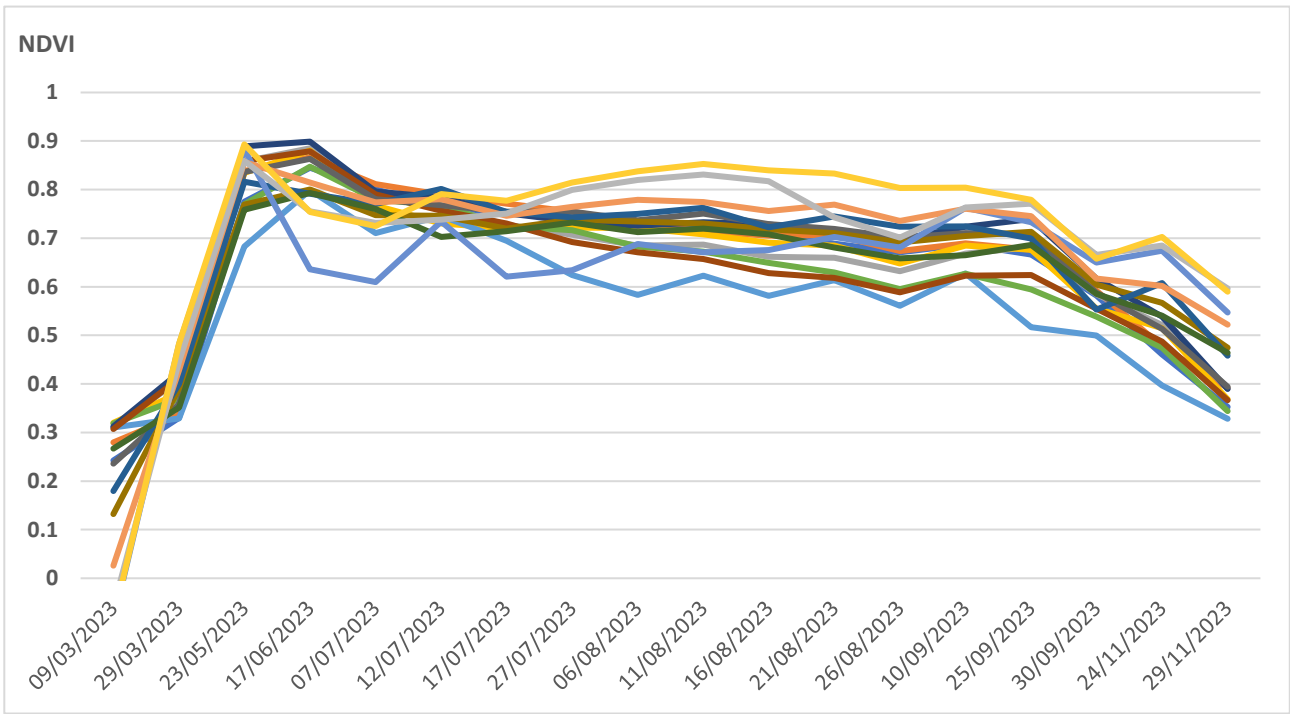


[Figure 26. NDVI Group 3 trend derived from cluster analysis]

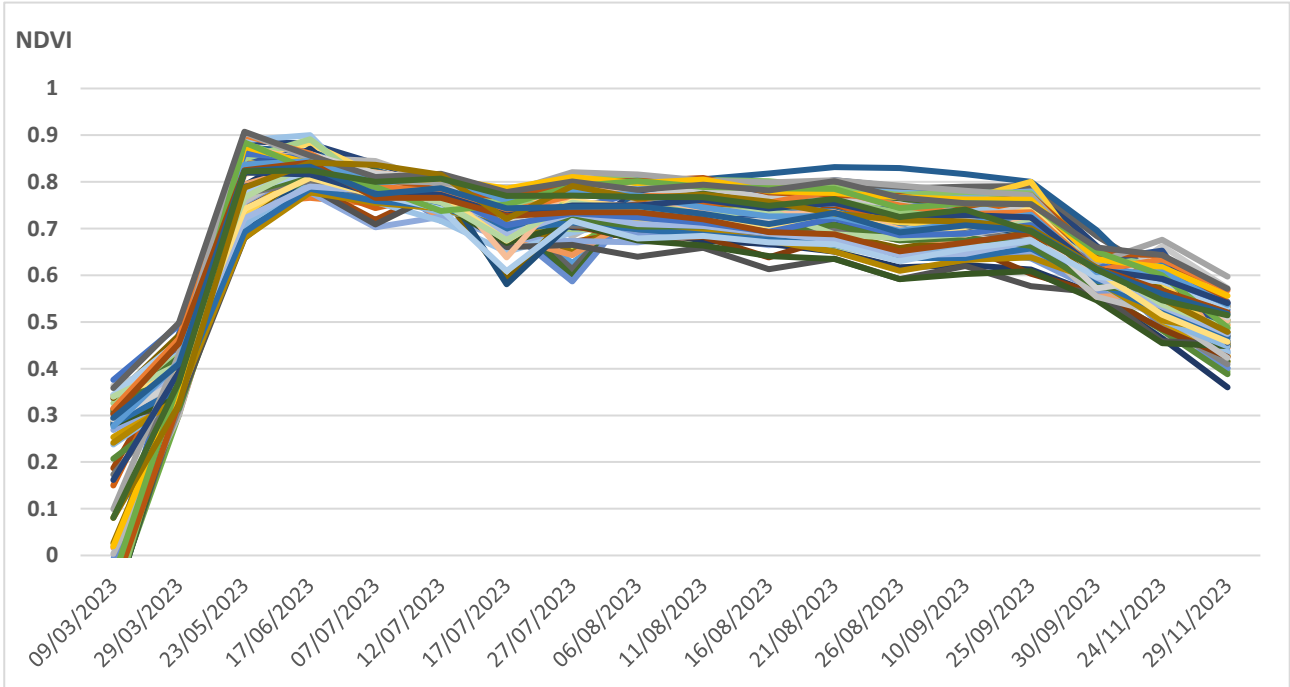


[Figure 27. NDVI Group 4 trend derived from cluster analysis]

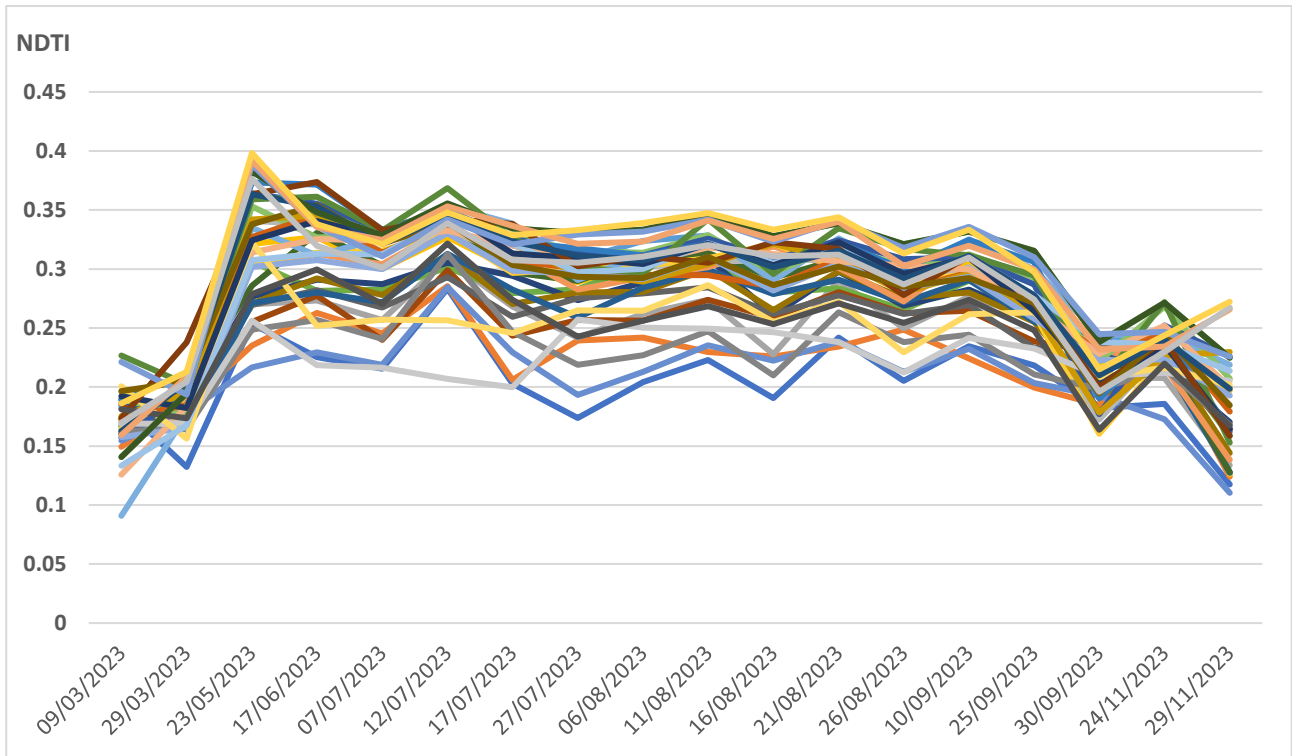


[Figure 28. NDTI Group 1 trend derived from cluster analysis]

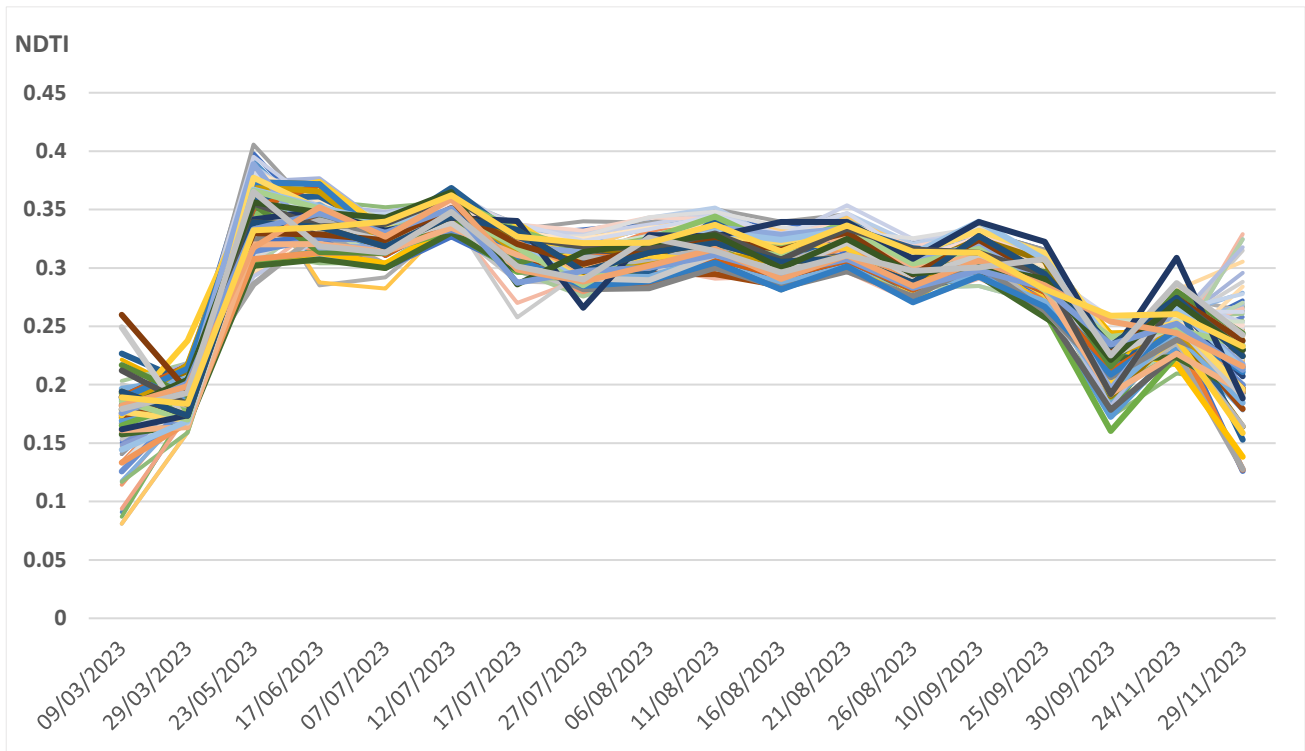


[Figure 29. NDTI Group 2 trend derived from cluster analysis]

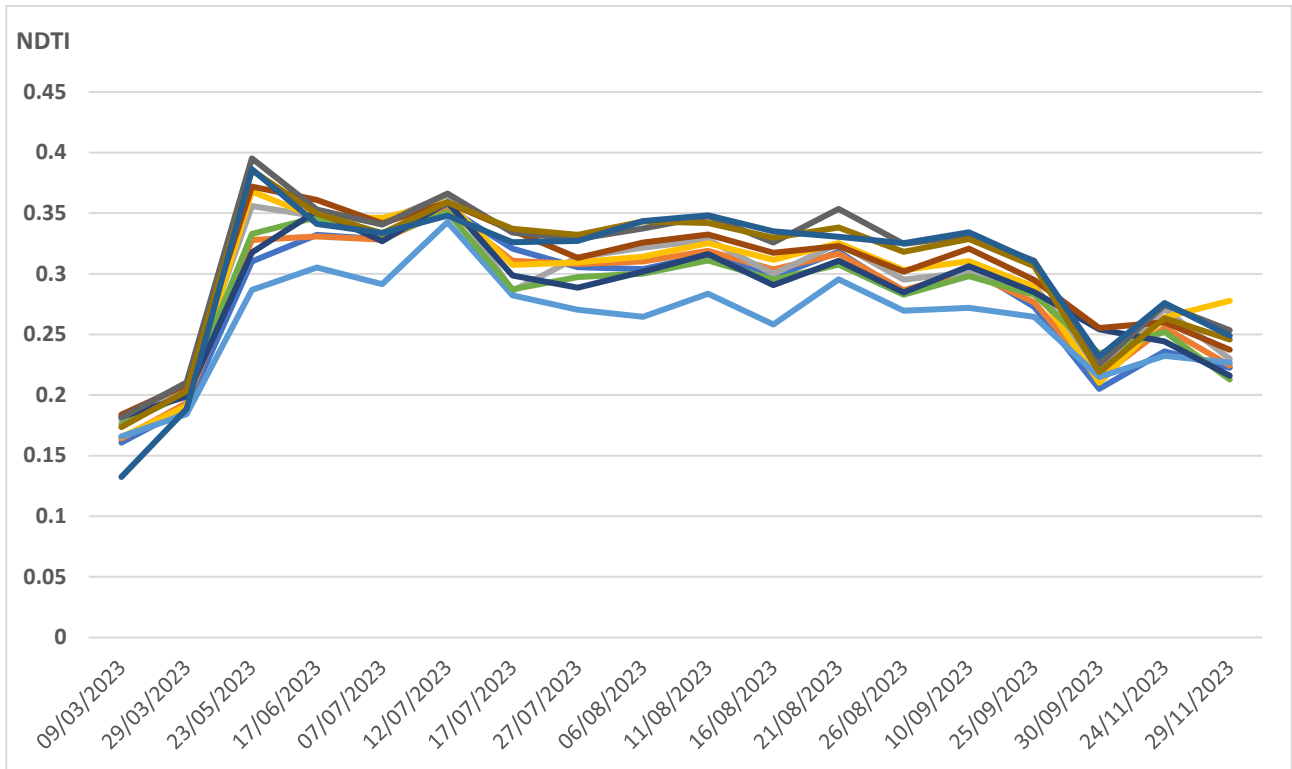


[Figure 30. NDTI Group 3 trend derived from cluster analysis]

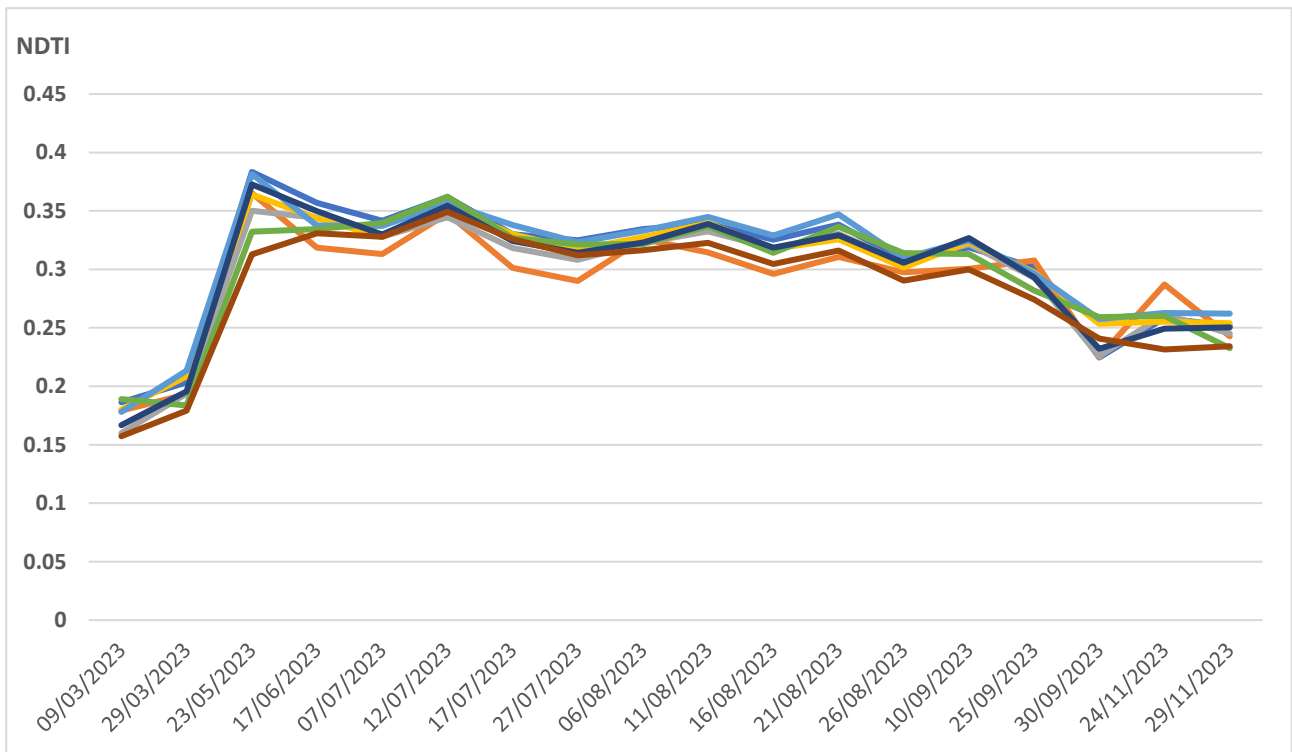


[Figure 31. NDTI Group 4 trend derived from cluster analysis]

BIBLIOGRAPHY

Adame-Campos R., Ghilardi A., Gao Y Variables Selection for Aboveground Biomass Estimations Using Satellite Data: A Comparison between Relative Importance Approach and Stepwise Akaike's Information Criterion, ISPRS International Journal of Geo-Information, 2019

Alford A., Griffith G., Livestock Farming Systems in the Northern Tablelands, NSW Agriculture, Economic Research Report No.12, 2003

Ali I., Cawkwell F., Dwyer E., Satellite remote sensing of grasslands: from observation to management, Journal of Plant Ecology, 2016

Andreatta D., Gianelle D., Scotton M., Dalponte M., Estimating grassland vegetation cover with remote sensing: A comparison between Landsat-8, Sentinel-2 and PlanetScope imagery, Ecological Indicators, Elsevier, 2022

Baghdadi, N., Mohammad, E.H., Mehrez, Z., 2016. Coupling SAR C-band and optical data for soil moisture and leaf area index retrieval over irrigated grasslands. Geoscience & Remote Sensing Symposium 3551–3554.

Baghi, N.G., Oldeland, J., Do soil-adjusted or standard vegetation indices better predict above ground biomass of semi-arid, saline rangelands in North-East Iran?, Remote Sens. 40 (22), 8223–8235, 2019

Bao, N., Li, W., Gu, X., Liu, Y., 2019. Biomass estimation for semiarid vegetation and mine rehabilitation using Worldview-3 and Sentinel-1 SAR imagery. Remote Sens. 11.

Barboza, T.O.C.; Ardiguieri, M.; Souza, G.F.C.; Ferraz, M.A.J.; Performance of Vegetation Indices to Estimate Green Biomass Accumulation in Common Bean. AgriEngineering 5-840–854, 2023.

Bareth, G.; Schellberg, J. Replacing Manual Rising Plate Meter Measurements with Low-Cost UAV-Derived Sward Height Data in Grasslands for Spatial Monitoring. PFG—J. Photogramm. Remote Sens. Geoinf. Sci. 2018, 86, 157–168.

Barrachina M., Cristobal J., Tulla A.F., Estimating above-ground biomass on mountain meadows and pastures through remote sensing, International Journal of Applied Earth Observation and Geoinformation, Elsevier, 2014

Bastiaanssen, W.G.M., David, J.M., Ian, W.M., 2000. Remote sensing for irrigated agriculture: examples from research and possible applications. Agric. Water Manag. 46 (2), 137–155.

Bayaraa B, Hirano A., Purevtseren M., Applicability of different vegetation indices for pasture biomass estimation in the north-central region of Mongolia, Geocarto International, 2022

Basso E., *Botanical composition and forage quality of a mountain pasture, University of Padova*, 2019

Bazzo, C.O.G.; Kamali, B.; Hütt, C.; Bareth, G.; Gaiser, T. A Kamali B., A Review of Estimation Methods for Aboveground Biomass in Grasslands Using UAV, MDPI, 2023.

- Bharti, A.; Paritosh, K.; Mandla, V.R.; GIS Application for the Estimation of Bioenergy Potential from Agriculture Residues: An Overview. *Energies* 14:898, 2021.
- Boschetti M., Bocchi S., Brivio P.A., Assessment of pasture production in the Italian Alps using spectrometric and remote sensing information, *Agriculture, Ecosystems & Environment*, Elsevier, 2006
- Carpintero E., Andreu A., Gómez-Giráldez P.J., Remote-Sensing-Based Water Balance for Monitoring of Evapotranspiration and Water Stress of a Mediterranean Oak–Grass Savanna, *MDPI Water*, 2020.
- Casanova, D., Epema, G.F., Goudriaan, J., 1998. Monitoring rice reflectance at field level for estimating biomass and LAI. *Field Crops Res.* 55, 83–92.
- Casanova, D., Epema, G.F., Goudriaan, J., 1998. Monitoring rice reflectance at field level for estimating biomass and LAI. *Field Crops Res.* 55, 83–92.
- Castle ME (1976) A simple disc instrument for estimating herbage yield. *J Br Grassl Soc* 31:37–40.
- Chen Y.; Guerschman, J.; Shendryk, Y.; Henry, D.; Harrison, M.T. Estimating Pasture Biomass Using Sentinel-2 Imagery and Machine Learning. *Remote Sens.* 2021
- Cheng, T., Song, R., Li, D., Zhou, K., Zheng, H., Yao, X., Tian, Y., Cao, W., Zhu, Y., Cheng, T., 2017. Spectroscopic estimation of biomass in canopy components of paddy rice using dry matter and chlorophyll indices. *Remote Sensing* 9, 319.
- Cleland, E.E., Chiariello, N.R., Loarie, S.R., Mooney, H.A., Field, C.B., 2006. Diverse responses of phenology to global changes in a grassland ecosystem. *Proc. Natl. Acad. Sci. USA* 103, 13740–13744.
- Del Pozo A, Ovalle C, Casado MA, Effects of grazing intensity in grasslands of the Espinal of central Chile. *J Veg Sci* 17:791–8, 2006.
- Enkhtuya J., Altangerel M., Damdinsuren A., ANALYSIS OF VEGETATION INDICES FOR PASTURE BIOMASS EVALUATION USING MULTI-TEMPORAL SATELLITE IMAGES AND UAV DATA, *ACRS Mongolia*, 2022
- Flores, A.N.; Ivanov, V.Y., Impact of hillslope-scale organization of topography, soil moisture, soil temperature, and vegetation on modeling surface microwave radiation emission. *IEEE Trans. Geosci. Remote Sens.* 47, 2557–2571, 2009.
- Flores, A.N.; Ivanov, V.Y.; Entekhabi, D.; Bras, R.L. Impact of hillslope-scale organization of topography, soil moisture, soil temperature, and vegetation on modeling surface microwave radiation emission. *IEEE Trans. Geosci. Remote Sens.* 2009, 47, 2557–2571.
- Foley JA, DeFries R, Asner GP, et al. (2005) Global consequences of land use. *Science* 309:570–74.
- Fu, Y., Yang, G., Wang, J., Song, X., Feng, H., 2014. Winter wheat biomass estimation based on spectral indices, band depth analysis and partial least squares regression using hyperspectral measurements. *Comput. Electron. Agric.* 100, 51–59.

- Gano, B.; Dembele, J.S.B.; Ndour, A.; Luquet, D., Using UAV Borne, Multi-Spectral Imaging for the Field Phenotyping of Shoot Biomass, Leaf Area Index and Height of West African Sorghum Varieties under Two Contrasted Water Conditions, *Agronomy* 2021.
- Gao, X.; Huete, A.R.; Ni, W.; Miura, T. Optical-biophysical relationships of vegetation spectra without background contamination. *Remote Sens. Environ.* 2000, 74, 609–620.
- Gargiulo J., Clark C., Lyons N., Spatial and Temporal Pasture Biomass Estimation Integrating Electronic Plate Meter, Planet CubeSats and Sentinel-2 Satellite Data, *MDPI Forest*, 2020.
- Garrouste E.L., Hansen A.J., Lawrence R.L., Using NDVI and EVI to Map Spatiotemporal Variation in the Biomass and Quality of Forage for Migratory Elk in the Greater Yellowstone Ecosystem, *MDPI Remote Sensing*, 2016
- Greer, M.J., Wilson, G.W.T., Hickman, K.R., Wilson, S.M., 2014. Experimental evidence that invasive grasses use allelopathic biochemicals as a potential mechanism for invasion: chemical warfare in nature. *Plant Soil* 385, 165–179.
- Hakl J, Hrevušová Z, Hejcman M, et al. (2012) The use of a rising plate meter to evaluate lucerne (*Medicago sativa* L.) height as an important agronomic trait enabling yield estimation. *Grass Forage Sci* 67:589–96.
- Han, X.; Thomasson, J.A.; Bagnall, G.C, Measurement and Calibration of Plant-Height from Fixed-Wing UAV Images. *Sensors* 18-4092, 2018
- Han, X.; Thomasson, J.A.; Bagnall, G.C.; Pugh, N.A.; Horne, D.W.; Rooney, W.L.; Jung, J.; Chang, A.; Malambo, L.; Popescu, S.C.; et al. Measurement and Calibration of Plant-Height from Fixed-Wing UAV Images. *Sensors* 2018, 18, 4092.
- Hansen, M.C., Potapov, P.V., Moore, R., Hancher, M., High-resolution global maps of 21st-century forest cover change. *Science* 342, 850–853, 2013
- Harris, R.B., 2010. Rangeland degradation on the Qinghai-Tibetan plateau: a review of the evidence of its magnitude and causes. *J. Arid Environ.*
- Hejcman M, Sochorová L, Pavlů V, et al. (2014) The Steinach Grassland Experiment: soil chemical properties, sward height and plant species composition in three cut alluvial meadow after decades-long fertilizer application. *Agric Ecosyst Environ* 184:76–87.
- Hill MJ (2004) Grazing agriculture - Managed Pasture, Grassland and Rangeland. In Ustin SL (ed). *Manual of Remote Sensing, Remote Sensing for Natural Resource Management and Environmental Monitoring*. New York: Wiley International, 449–530.
- Holmes CW, Wilson GF, Mackenzie DDS, Flux DS, Brookes IM, Davey AWF (Ed. D Swain (2007) 'Milk production from pasture.' (Massey University: Palmerston North, New Zealand).
- Huete, A. R. 1988. "A Soil-Adjusted Vegetation Index (SAVI)." *Remote Sensing of Environment* 25 (3): 295–309.
- Huete, A.; Didan, K.; Miura, T.; Rodriguez, E.P.; Gao, X.; Ferreira, L.G. Overview of the radiometric and biophysical performance of the MODIS vegetation indices. *Remote Sens. Environ.* 2002, 83, 195–213.

- Jiang, Z.; Huete, A.R.; Didan, K.; Miura, T. Development of a two-band enhanced vegetation index without a blue band. *Remote Sens. Environ.* 112, 3833–3845, 2008.
- Jin Y., Yang X., Remote Sensing-Based Biomass Estimation and Its Spatio-Temporal Variations in Temperate Grassland, Northern China, *Remote Sensing*, 2014
- Johnson B., Tateishi R., Kobayashi T., Remote Sensing of Fractional Green Vegetation Cover Using Spatially-Interpolated Endmembers, *Remote Sensing*, 2012
- Kaliraj Seenipandi ¹, K.K. Ramachandran , Seasonal variability of sea surface temperature in Southern Indian coastal water using Landsat 8 OLI/TIRS images, Elsevier, 2021
- Klemas, V., 2013. Remote sensing of coastal wetland biomass: an overview. *J. Coastal Res.* 290, 1016–1028.
- Kwon, H.-Y., Nkonya, E., Johnson, T., Graw, V., Kato, E., Kihui, E., 2016. Global estimates of the impacts of grassland degradation on livestock productivity from 2001 to 2011. In: Nkonya, E., Mirzabaev, A., von Braun, J. (Eds.), *Economics of Land Degradation and Improvement – A Global Assessment for Sustainable Development*. Springer International Publishing, Cham, pp. 197–214.
- Latham J., Cumani R., Rosati I., Bloise M., 2014. Global Land Cover SHARE (GLC-SHARE): Database BetaRelease Version 1.0-2014.
- Lawrence RL, Ripple WJ. Comparisons among vegetation indices and bandwise regression in a highly disturbed, heterogeneous landscape: Mount St. Helens, Washington. *Rem Sens Environ*, 1998
- Le, Q.B., Nkonya, E., Mirzabaev, A., 2016. Biomass productivity-based mapping of global land degradation hotspots. In: Nkonya, E., Mirzabaev, A., von Braun, J. (Eds.), *Economics of Land Degradation and Improvement – A Global Assessment for Sustainable Development*. Springer International Publishing, Cham, pp. 55–84.
- Li Z., Guo X., A suitable vegetation index for quantifying temporal variation of leaf area index (LAI) in semiarid mixed grassland, *Remote Sensing*, Vol. 36, No. 6, pp. 709–721, 2010
- Li, T., Cui, L., Scotton, M., Dong, J., Xu, Z., Characteristics and trends of grassland degradation research. *J. Soils Sediments* 22 (7), 1901–1912, 2022
- Li, Z.W., Wang, J.H., Tang, H., Predicting grassland leaf area index in the meadow steppes of Northern China: a comparative study of regression approaches and hybrid geostatistical methods. *Remote Sens.-Basel* 8, 2016.
- Liang, S., & Wang, J., Fractional vegetation cover. In Academic Press (Ed.), *Advanced Remote Sensing (Second edi*, pp. 477–510), 2022
- Liu, H.Q.; Huete, A. A feedback-based modification of the NDVI to minimize canopy background and atmospheric noise. *IEEE Trans. Geosci. Remote Sens.* 1995, 33, 457–465.
- Ma, H., Mo, L., Crowther, T.W., Maynard, D.S., The global distribution and environmental drivers of aboveground versus belowground plant biomass. *Nat. Ecol. Evol.* 5, 1110–1122, 2021.
- Maes WH, Steppe K. Perspectives for Remote Sensing with Unmanned Aerial Vehicles in Precision Agriculture. *Trends Plant Sci.* 2019; 24.

- Matsushita, B., Yang, W., Chen, J., Onda, Y., Qiu, G., 2007. Sensitivity of the Enhanced Vegetation Index (EVI) and Normalized Difference Vegetation Index (NDVI) to Topographic Effects: A Case Study in High-Density.
- Meshesha D.T., Ahmed M.M., Prediction of grass biomass from satellite imagery in Somali regional state, eastern Ethiopia, Heliyon Cell Press, 2020.
- Michael McInerney, Robert Lozar, COMPARISON OF METHODOLOGIES TO DERIVE A NORMALIZED DIFFERENCE THERMAL INDEX (NDTI) FROM ATLAS IMAGERY, ASPRS 2007 Annual Conference.
- Michael McInerney, Robert Lozar, DERIVING A NORMALIZED DIFFERENCE THERMAL INDEX (NDTI) FROM ASTER SATELLITE IMAGERY, ASPRS 2008 Annual Conference
- Morais, T.G.; Teixeira, R.F.M.; Figueiredo, M.; Domingos, T. The Use of Machine Learning Methods to Estimate Aboveground Biomass of Grasslands: A Review. *Ecol. Indic.* 2021, 130, 108081.
- Motohka T., Nasahara K.N., Oguma H., Applicability of Green-Red Vegetation Index for Remote Sensing of Vegetation Phenology, *MDPI Remote Sensing*, 2010
- Munyati C., Detecting the distribution of grass aboveground biomass on a rangeland using Sentinel-2 MSI vegetation indices, *Advances in Space Research*, Elsevier, 2021
- Newnham G (2010) Improved Methods for Assessment and Prediction of Grassland Curing. *Satellite Based Curing Methods and Mapping - Final Report: Project A1.4.*
- Pettorelli, N.; Ryan, S.; Mueller, T.; Bunnefeld, N., Difference Vegetation Index (NDVI): Unforeseen successes in animal ecology. *Clim. Res.* 46, 15–27, 2011
- Pettorelli, N.; Ryan, S.; Mueller, T.; Bunnefeld, N.; Jedrzejewska, B.; Lima, M.; Kausrud, K. The Normalized Difference Vegetation Index (NDVI): Unforeseen successes in animal ecology. *Clim. Res.* 2011, 46, 15–27.
- Porter T.F., Chen C., Long J.A., Lawrence R.L., Sowell B.F., Estimating biomass on CRP pastureland: A comparison of remote sensing techniques, *Biomass and Bioenergy*, Elsevier, 2014
- Pullanagari R, Dynes R.A, King W.M., Assessment and impact of grass and forage quality, 2013
- Qi, J., A. Chehbouni, A. R. Huete, Y. H. Kerr, and S. Sorooshian. 1994. "A Modified Soil Adjusted Vegetation Index." *Remote Sensing of Environment* 48 (2): 119–126.
- Qin Q. , Xu D. , Hou L. , Shen B., Comparing vegetation indices from Sentinel-2 and Landsat 8 under different vegetation gradients based on a controlled grazing experiment, *Ecological Indicators*, Elsevier, 2021
- Ronchi B., Primi R., Remote sensing for real time estimate of aboveground biomass productivity in mountain pasture, *Options Méditerranéennes* 2019
- Rondeaux, G., M. Steven, and F. Baret. 1996. "Optimization of Soil-Adjusted Vegetation Indices." *Remote Sensing of Environment* 55 (2): 95–107.

Rouse, J.W.; Haas, R.H.; Schell, J.A.; Monitoring Vegetation Systems in the Great Plains with ERTS. In Proceedings of the 3rd ERTS Symposium, Washington, DC, USA, 10–14, 1974

Salvan D., *Proximity remote sensing for estimating the spatio-temporal variability of the vegetation of grasslands*, University of Padova, 2022

Schellberg, J., Verbruggen, E., Frontiers and perspectives on research strategies in grassland technology. *Crop and Pasture Science* 65 (6), 508, 2014

Scurlock, J.M.O., Hall, D.O., The global carbon sink: a grassland perspective. *Glob. Change Biol.* 4 (2), 229–233, 1998

Shahbazi M, Theau J, Menard P. Recent applications of unmanned aerial imagery in natural resource management. *GISci. Remote Sens.* 2014; 51: 339–365.

Shen A., Wu C., Jiang B., *Spatiotemporal Variations of Aboveground Biomass under Different Terrain Conditions*, MDPI Forest, 2018

Shoko, C., Mutanga, O., Dube, T., 2016. Progress in the remote sensing of C3 and C4 grass species aboveground biomass over time and space. *Isprs J. Photogramm.* 120, 13–24.

Silleos a; Thomas K. Alexandridis a; Ioannis Z. Gitas b; Konstantinos, Perakis *Vegetation Indices: Advances Made in Biomass Estimation and Vegetation Monitoring in the Last 30 Years*, Geocarto International, 2006.

Singh C., Karan S.H., Sardar P., Remote sensing-based biomass estimation of dry deciduous tropical forest using machine learning and ensemble analysis, *Journal of Environmental Management*, Elsevier, 2022.

Somvanshi S.S., Kumari M., Comparative analysis of different vegetation indices with respect to atmospheric particulate pollution using sentinel data, *Applied Computing and Geosciences*, Elsevier, 2020

Su, W.; Zhang, M.; Bian, D.; Liu, Z.; Huang, J.; Wang, W.; Wu, J.; Guo, H. Phenotyping of corn plants using unmanned aerial vehicle (UAV) images. *Remote Sens.* 2019, 11, 2021.

Theau J, Lauzier-Hudon E', Estimation of forage biomass and vegetation cover in grasslands using UAV imagery, *Plos one*, 2021.

Tittebrand, A.; Spank, U.; Bernhofer, C.H. Comparison of satellite and ground-based NDVI above different land-use types. *Theor. Appl. Climatol.* 2009, 98, 171–186.

Trentin, C.B.; Trentin, A.B.; Saldanha, D.L. Relação entre a biomassa da vegetação campestre nativa e dados de sensoriamento remoto orbital. *Geographia* 2019, 21, 98.

Tucker, C.J. Asymptotic nature of grass canopy spectral reflectance. *Appl. Opt.* 1977, 16, 1151–1156.

Ulyatt M (1973) The feeding value of herbage. *Chemistry and biochemistry of herbage* 3, 131-178.

Wang J., Xiao X., Estimating leaf area index and aboveground biomass of grazing pastures using Sentinel-1, Sentinel-2 and Landsat images, *ISPRS Journal of Photogrammetry and Remote Sensing*, Elsevier, 2019.

Wang, Y., Zhang, K., Tang, C., Cao, Q., Tian, Y., Zhu, Y., Cao, W., Liu, X., 2019. Estimation of rice growth parameters based on linear mixed-effect model using multispectral images from fixed-wing unmanned aerial vehicles. *Remote Sens.* 11.

Xiao, C., Li, P., Feng, Z., Liu, Y., Zhang, X., Sentinel-2 red-edge spectral indices (RESI) suitability for mapping rubber boom in Luang Namtha Province, northern Lao PDR. *Int. J. Appl. Earth Obs. Geoinf.* 93, 2020.

Xie Y, Sha Z, Yu M, et al. (2009) A comparison of two models with Landsat data for estimating above ground grassland biomass in Inner Mongolia, China. *Ecol Model* 220:1810–8.

Xu B, Yang XC, Tao WG, et al. (2008) MODIS-based remote sensing monitoring of grass production in China. *Int J Remote Sens* 29:5313–27.

Xue J., Su B., Significant Remote Sensing Vegetation Indices: A Review of Developments and Applications, Hindawi Journal of Sensors, 2017.

Yu, R., Evans, A.J., Malleson, N., 2018. Quantifying grazing patterns using a new growth function based on MODIS leaf area index. *Remote Sens. Environ.* 209, 181–194.

Zhang, J.; Gao, H.; Ying, B.; Wang, J.; Yuan, W.; Zhu, J.; Yi, L.; Jiang, B. The biomass dynamic analysis of public waifare forest in Xianju county of Zhejiang province. *J. Nanjing For. Univ. (Nat. Sci. Ed.)* 2011, 35, 147–150.

Zhang, J.; Gao, H.; Ying, B.; Wang, J.; Yuan, W.; Zhu, J.; Yi, L.; Jiang, B. The biomass dynamic analysis of public waifare forest in Xianju county of Zhejiang province. *J. Nanjing For. Univ. (Nat. Sci. Ed.)* 2011, 35, 147–150.

Zhang, J.; Gao, H.; Ying, B.; Wang, The biomass dynamic analysis of public waifare forest in Xianju county of Zhejiang province. *J. Nanjing For. Univ. (Nat. Sci. Ed.)*, 35, 147–150, 2011.

Zhou, H., Zhao, X., Tang, Y., Alpine grassland degradation and its control in the source region of the Yangtze and Yellow Rivers. *China. Grassl. Sci.* 51, 191–203, 2005.

Zhou, H., Zhao, X., Tang, Y., Gu, S., Zhou, L., 2005. Alpine grassland degradation and its control in the source region of the Yangtze and Yellow Rivers. *China. Grassl. Sci.* 51, 191–203.

WEBSITES

www.apps.dtic.mil

www2.arpa.veneto.it

www.dlf.ie

www.fao.org

www.laviadellemalghe.it

www.mla.com

www.tirolo.com

This study was carried out within the Agritech National Research Center and received funding from the European Union Next-Generation EU (PIANO NAZIONALE DI RIPRESA E RESILIENZA (PNRR) – MISSIONE 4 COMPONENTE 2, INVESTIMENTO 1.4 – D.D. 1032 17/06/2022, CN00000022). This thesis reflects only the author's, supervisors', and co-supervisors' views and opinions; neither the European Union nor the European Commission can be considered responsible for them.